

# SIMULTANEOUS RECONSTRUCTION OF SPATIAL FREQUENCY FIELDS AND SAMPLE LOCATIONS VIA BAYESIAN SEMI-MODULAR INFERENCE

BY CHRIS U. CARMONA<sup>1</sup>, ROSS A. HAINES<sup>3</sup>, MAX ANDERSON LOAKE<sup>1,\*</sup>,  
MICHAEL BENSKIN<sup>2</sup> AND GEOFF K. NICHOLLS<sup>1,†</sup>

<sup>1</sup>DEPARTMENT OF STATISTICS, UNIVERSITY OF OXFORD, CCARMONA@BERKELEY.EDU;  
<sup>\*</sup>MAX.ANDERSONLOAKE@KEBLE.OX.AC.UK; <sup>†</sup>NICHOLLS@STATS.OX.AC.UK

<sup>2</sup>DEPARTMENT OF LITERATURE, AREA STUDIES AND EUROPEAN LANGUAGES, UNIVERSITY OF OSLO,  
MICHAEL.BENSKIN@ILOS.UIO.NO

<sup>3</sup>PALANTIR TECHNOLOGIES, ROSS.A.HAINES@GMAIL.COM

Traditional methods for spatial inference estimate smooth interpolating fields based on features measured at well-located points. When the spatial locations of some observations are missing, joint inference of the fields and locations is possible as the fields inform the locations and *vice versa*. If the number of missing locations is large, conventional Bayesian Inference fails if the generative model for the data is even slightly mis-specified, due to feedback between estimated fields and the imputed locations. Semi-Modular Inference (SMI) offers a solution by controlling the feedback between different modular components of the joint model using a hyper-parameter called the influence parameter. Our work is motivated by linguistic studies on a large corpus of late-medieval English textual dialects. We simultaneously learn dialect fields using dialect features observed in “anchor texts” with known location *and* estimate the location of origin for “floating” textual dialects of unknown origin. The optimal influence parameter minimises a loss measuring the accuracy of held-out anchor data. We compute a (flow-based) variational approximation to the SMI posterior for our model. This allows efficient computation of the optimal influence. MCMC-based approaches, feasible on small subsets of the data, are used to check the variational approximation.

**1. Introduction.** In the conventional setting of *point-referenced data* (Banerjee, Carlin and Gelfand, 2014), data are vectors  $y_p \in \mathcal{Y}$ ,  $p \in A$ ,  $A = \{1, 2, \dots, N\}$  measured at fixed locations  $x_p \in \mathcal{X}$  in a region  $\mathcal{X} \subseteq \mathbb{R}^2$ , collectively  $X_A = (x_p)_{p \in A}$  and  $Y_A = (y_p)_{p \in A}$ . Statistical methods commonly assume that the locations are known and specify a hierarchical generative model, assuming that data at  $x \in \mathcal{X}$  are generated conditional on the local value  $\Phi(x)$  of a multi-dimensional latent spatial field  $\Phi : \mathcal{X} \rightarrow \mathbb{R}^{d_\phi}$ . Allowing other global parameters  $\theta$ , the observation model has the form

$$y_p \sim P(\cdot | \Phi(x_p), \theta), \quad p \in A.$$

Let  $\Phi(X_A) = (\Phi(x_p))_{p \in A}$  give the field values at the observation locations. A Bayesian approach assigns prior distributions to the latent fields and global parameters, and targets the posterior distribution conditional on these “anchor” data,

$$P(\Phi(X_A), \theta | Y_A) \propto P(Y_A | \Phi(X_A), \theta) P(\Phi(X_A), \theta).$$

---

*Keywords and phrases:* Generalized Bayesian Inference, Modular Inference, Cutting feedback, Variational Methods, Gaussian Processes.

There is a large literature for this setting with known locations, covering different specifications for the response vector and prior. However, few methods have been developed to handle the situation in which some sample locations are missing and estimation of these locations is the goal.

Suppose that we are given an additional set of  $M$  measurements  $y_p$ ,  $p \in \bar{A}$ ,  $\bar{A} = \{N + 1, \dots, N + M\}$  with unknown locations. We call these data “floating” data  $Y_{\bar{A}} = (y_p)_{p \in \bar{A}}$  and the data  $y_p$ ,  $p \in A$  “anchor data” and assume the floating and anchor data are realisations of a common generating process. The observed data is then  $X_A, Y_A, Y_{\bar{A}}$ . The missing locations of floating data,  $X_{\bar{A}} = (x_p)_{p \in \bar{A}}$ , enter as unknown quantities in the model. Let  $\mathcal{P} = A \cup \bar{A}$ , let  $X_{\mathcal{P}} = (X_A, X_{\bar{A}})$  be the set of all locations for observations, known and unknown and let  $Y_{\mathcal{P}} = (Y_A, Y_{\bar{A}})$ . The posterior distribution is now

$$P(\Phi(X_{\mathcal{P}}), \theta, X_{\bar{A}} | Y_{\mathcal{P}}) \propto P(Y_A | \Phi(X_A), \theta) P(Y_{\bar{A}} | \Phi(X_{\bar{A}}), \theta) P(\Phi(X_{\mathcal{P}}), \theta, X_{\bar{A}}).$$

where  $\Phi(X_{\mathcal{P}}) = (\phi(x_p))_{p \in \mathcal{P}}$  are the values of the multidimensional latent field at all locations.

The first contribution of this work is to provide a statistical framework to estimate the missing locations  $x_p \in \bar{A}$  jointly with estimation of the fields  $\Phi$ . Bayesian inference for missing locations is explored in Giorgi and Diggle (2015). They develop an MCMC procedure to target missing locations in a rectangular region in  $\mathbb{R}^2$ , assuming normally distributed observations with a single spatial field parameterising the mean. They focus on cases where the number of floating observations is at most two. One important challenge in our setting is the sparsity of the data vectors  $y_p$ ,  $p \in \mathcal{P}$  and the high dimension of  $\Phi$ . In the model below, the fields  $\Phi$  are represented using Gaussian Processes. Using a softmax transformation, each component field in  $\Phi$  parameterises the probability to select one level of one categorical variable. This is the GP-Generalized Linear Model (GLM) modelling framework of Diggle, Tawn and Moyeed (1998); Savitsky, Vannucci and Sha (2011). We have observations of 71 categorical variables at each location in our main analysis, and each categorical variable has many levels, so we have hundreds of spatial fields.

This data-sparsity is a distinctive feature of the model: if we take measurements of an additional categorical variable at each location, we add a set of fields for each level of the new variable. If we add data in this way, we increase the dimension of the parameter space significantly. However, if we add new anchor measurements  $x_p, y_p$  to  $A$ , keeping the number of variables observed at each location fixed (so fixed dimension for  $\Phi$ ), then under regularity conditions and in the well-specified setting we expect the fields to concentrate on their true values. Consistency results for the unknown locations  $X_{\bar{A}}$  of the floating observations are outside the scope of our work; we plot marginal posterior distributions for locations based on the data we actually have.

When the fields are informed by sparse and indirect measurements, and just a subset of those observations are anchors, the analysis is exposed to mis-specification, and this motivates our use of specialised methods for handling model mis-specification; extending these methods to work in our setting is a second contribution of this paper. In a straightforward Bayesian analysis the posterior distribution for the unknown locations  $X_{\bar{A}}$  and latent fields  $\Phi(X_{\mathcal{P}})$  appear in a single joint distribution conditioned on the known locations  $X_A$  and the response data  $Y_{\mathcal{P}}$ . In this setting response data  $Y_{\bar{A}}$  measured at unknown locations also inform, or “feed-back”, into the posterior distribution for latent fields. If the number  $M$  of observations with missing locations is large compared to the number  $N$  of observations with known locations, and the model is mis-specified, then this feedback can pose real problems: incorrect locations may distort the field posterior, which in turn biases location estimates.

In an analysis of the same data, Haines (2016) gets around this problem by restricting analysis to a subset of the data and reducing the number of float locations, but this is unsatisfactory. Model elaboration (Gelman et al., 2015) helped, and we present here our best post-elaboration model, a significant improvement over that given in Haines (2016). However, goodness of fit problems remain as we show below.

Bayesian inference in the  $\mathcal{M}$ -open setting, where the true generative model is not in the class of models expressed by the prior and likelihood, has progressed a great deal in the last decade (Zhang, 2006; Liu, Bayarri and Berger, 2009; Plummer, 2015; Bissiri, Holmes and Walker, 2016; Grünwald and Ommen, 2017; Carmona and Nicholls, 2020). The approach we take, based on Bayesian Multiple Imputation (BMI), draws on this literature. BMI can be understood as a two-stage inferential process. First, in an *imputation stage*, the posterior distribution for the unknown spatial fields and background parameters is formed using the anchor data alone. Then in a second *analysis stage*, the posterior for float locations is conditioned on the measurements at those locations and the imputed field distributions. The imputed fields are random variables passed from the imputation to the analysis, hence the BMI designation. This two-stage approach to estimation of missing observation-locations was taken in Wasser et al. (2004, 2007). Although this approach has many Bayesian elements, it does not define a standard Bayesian posterior.

In the Bayesian Multiple Imputation setup, feedback from float locations into field estimates is “cut”, so we call the resulting joint “posterior distribution” a *Cut posterior* (Liu, Bayarri and Berger, 2009; Plummer, 2015). However, in mildly mis-specified settings, completely cutting feedback may be unnecessarily conservative and some scheme allowing some controlled feedback from floating locations into field estimates may do better. In this paper we “select the inference” (Jacob et al., 2017) in a single overarching framework called Semi-Modular Inference (SMI) (Carmona and Nicholls, 2020, 2022; Nicholls et al., 2022). This includes Cut-model inference and Bayesian inference as special cases. Sampling an SMI- or Cut-posterior using Monte Carlo methods is more challenging than sampling the equivalent standard Bayesian posterior distribution (Plummer, 2015; Liu and Goudie, 2022a), and may require two-stage MCMC methods (Jacob, O’Leary and Atchadé, 2020) or variational approximations (Yu, Nott and Smith, 2021; Carmona and Nicholls, 2022).

The generative model we write down for for the float locations, background parameters, fields and observations is developed from the model given in Haines (2016). That work introduces the data and develops models in more detail than we do here. It gives comparisons with alternative methods including  $k$ -Nearest Neighbours. These are not competitive with Cut posterior inference, though Nearest Neighbours shows promise. We refer the reader to Haines (2016) for these experiments.

**2. The Linguistic Atlas of Late Mediaeval English (LALME) Data.** We now describe the data in detail. See appendix A in the Supplementary Material for further background from the perspective of historical linguistics and Haines (2016) for exploration of these data from a statistical perspective.

The Linguistic Atlas of Late Mediaeval English (LALME), originally published by McIntosh, Samuels and Benskin (1986) and later revised and supplemented by Benskin and Laing (Benskin et al., 2013), provides a corpus of lexico-grammatical data across a range of late mediaeval texts. The Atlas is founded on inventories of spellings from 1044 text samples selected from over 5000 source documents written in England, parts of Wales, and a small number from southern Scotland, and spans approximately 1350CE to 1450CE. Where a selected source is written by more than one scribe, the source is

segmented into multiple text samples, by handwriting, so that each each inventory, a "linguistic profile", records the usage of an individual scribe, at a time when spelling practice was still local in the main: a national written standard was coming into being only towards the end of the period. Local or regional variation in part reflects spoken language – "scribes spelled as they spoke" – but conventions of writing independent of speech may no less be markers of a scribe's local origins (Benskin, 1982) The linguistic profiles are completed survey questionnaires, and the questionnaire, in fixed format, is designed to elicit data of both kinds.

Each category in the questionnaire is an *item* (loosely, a separate word or grammatical element, indicated by  $\{\}$ ), which elicits the *forms* (loosely, different spellings, indicated below by  $\langle \rangle$ ) functionally equivalent to that item. We elaborate these definitions in appendix A.3. For example, the item  $\{\text{AGAINST}\}$  has 165 variant forms, including  $\langle \text{AGEINST} \rangle$ ,  $\langle \text{AYEINST} \rangle$ ,  $\langle \text{AGAINz} \rangle$  and  $\langle \text{TOYENST} \rangle$  (lower case letters are used for manuscript symbols, abbreviations and mediaeval letters now obsolete). A single item can have many forms, some as many as several hundred. The Atlas authors start with a list of items. They have  $P$  sample texts and take each text and go through each item in the list recording the forms of the item which appear in the text. Each text is then summarised by a record called a Linguistic Profile (LP) recording for each item the forms it contains.

Denote by  $\mathcal{I} = \{1, 2, \dots, I\}$  the set of all item labels (distinct words and grammatical concepts) and for each item  $i \in \mathcal{I}$  let  $\mathcal{F}_i = \{1, 2, \dots, F_i\}$  give the set of forms it takes. For example if  $i \in \mathcal{I}$  is the item label for  $\{\text{AGAINST}\}$  then each of the forms listed above will have a corresponding label  $f \in \mathcal{F}_i$ . As explained below, we focus on  $I = 71$  selected forms which we subject to re-registration in a linguistically informed coarsening process detailed below and in appendix A.4. There are in all  $d_\phi = \sum_{i=1}^I F_i$  forms in these data. Let  $\mathcal{P} = \{1, 2, \dots, P\}$  give the set of profile labels. An observation  $y_{p,i,f} = 1$  indicates that form  $f$  of item  $i$  is present in the sample text summarised by profile  $p$ , and  $y_{p,i,f} = 0$  is observed otherwise. Let  $y_{p,i} = (y_{p,i,f})_{f \in \mathcal{F}_i}$  and  $y_p = (y_{p,i})_{i \in \mathcal{I}}$ , so that data  $y_p \in \{0, 1\}^{d_\phi}$  records the presence and absence of forms for the LP for the text with label  $p \in \mathcal{P}$ .

The 1044 LPs are divided into two categories: anchor profiles and floating profiles. Anchor profiles are localised on the basis of non-linguistic evidence. In rare cases, a scribe with known biography can be identified, but most anchors are relatively short legal or administrative documents whose place of origin is explicitly stated. In such cases the text is assumed (if there is no evidence to the contrary) to represent the local forms of language. McIntosh, Samuels and Benskin (1986) deduce the location of floating profiles using a sequential method they call the *fit-technique*. This is described in more detail in appendix A.2, what follows is an outline. For each form that appears in a floating profile, anchor profiles and previously located floating profiles are used to delimit the region in which this form was used. The unknown profile location should lie in the intersection of all such regions across all the forms that the floating profile displays. A profile that cannot be localised in this way is likely to represent a dialect mixture; in many cases such mixtures result from uneven copying from a text written in a dialect that is not the scribe's own. (Benskin and Laing, 1981) The localised float is then treated as an anchor and the process continued until all the floats are positioned. If someone wishes to locate a new text they treat it as the  $M + 1$ 'st float and apply the same method.

Statistical modelling of these data is challenging, as a given item can have hundreds of forms, and many of these may be rare. In order to treat this a coarsened version of the data was made. This coarsening is described in appendix A.4. Forms with very similar spellings were merged according to linguistic criteria developed by the authors

of the Atlas. The coarsened data contains, for the purpose of location estimation, most of the information in the original data, but is significantly less sparse. In this paper we analyse the coarsened data.

We focus on a rectangular region, displayed in fig. 1, spanning 200 km east-west and 180 km north-south. The region contains  $N = 120$  anchor profiles with labels  $A = \{1, \dots, N\}$ . A further  $M = 247$  floating profiles with labels  $\bar{A} = \{N + 1, \dots, N_M\}$  were assigned to this region using the fit-technique (so that  $P = 367$  above). We are assuming the Atlas float-locations are sufficiently accurate for this purpose. Our analysis below supports this, so the selection rule and analysis results are at least consistent. The data  $X_A, Y_A, Y_{\bar{A}}$  and missing data  $X_{\bar{A}}$  are now as defined in the introduction. There are in all  $d_\phi = 741$  forms in the coarsened data displayed in the region of interest. As an example of dialectal variation, in fig. 2 we display the locations corresponding to usage of coarsened forms of the item {SUCH}.

The third contribution of our work is our analysis of the Atlas data itself. We estimate and quantify uncertainty in the location of floating profiles given the anchor profiles. This is the same problem the Atlas authors faced. We get good agreement between the credible regions we estimate for floating profiles and the Atlas locations estimated using the fit-technique. Our approach is automated, and provides well-calibrated uncertainty measures for location. The level of location precision achievable with these data has been in question and this is not easily quantified using the non-statistical fit-technique. Our analysis shows that location accuracy of order thirty kilometres is possible, underpinning the value of the Atlas. One application of the Atlas is to locate new floating profiles. We validate our method by treating anchors as if they were floating profiles and predicting their locations. This demonstrates the feasibility of locating new texts.

### 3. Methodology.

3.1. *Gaussian Processes for Latent Fields.* Gaussian Processes (GPs) (Rasmussen and Williams, 2005) form a flexible prior over functions and have been used to model latent spatial fields (Diggle et al., 2013; Lloyd et al., 2015; Aglietti et al., 2019). Bayesian inference for indirectly observed latent spatial fields using GPs gives well calibrated measures of uncertainty when the prior and observation models are well specified.

We have a large number of spatial fields in our motivating problem, reaching many hundreds. Moreover, fields representing different forms of a given item (some particular word) are anti-correlated at each location: if one spelling of a word is common at some location then other spellings are typically uncommon. However, frequencies of spellings of different words are expected to be correlated by shared dialect: similar patterns of spelling preferences across different words recur at different locations. In order to capture correlation between intensity fields and improve scalability on the dictionary dimension, we follow the Linear Model of Coregionalization (LMC) (Journal and Huijbregts, 1978; Álvarez, Rosasco and Lawrence, 2012) in which a large number of fields are given as different linear combinations of a small number of basis fields.

In order to improve scalability with increasing numbers of profiles and to make variational inference more straightforward, we use a sparse approximation to the fields via inducing points (Titsias, 2009; Bonilla, Krauth and Dezfouli, 2019; Quiñonero-Candela and Rasmussen, 2005). Inducing values augment the prior specification and serve as *global parameters* that are convenient for approximating the posterior distribution of the entire field via Stochastic Variational Inference (SVI) (Hensman, Fusi and Lawrence, 2013; Hensman, Matthews and Ghahramani, 2015). We treat the field values at inducing points as random variables in the posterior and marginalise (approximately) over

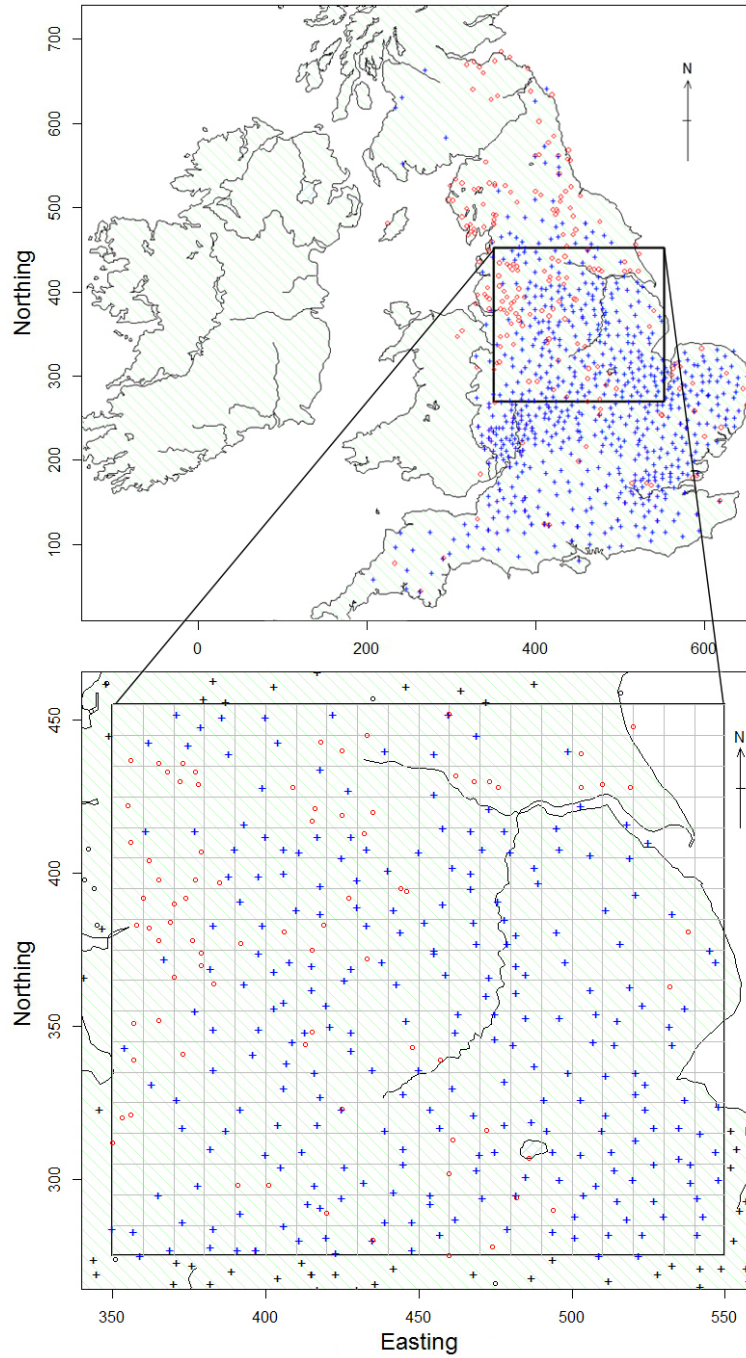


Figure 1: The locations of the anchor profiles (red) and the locations of the floating profiles estimated using the fit-technique (blue). We focus on a  $200 \text{ km} \times 180 \text{ km}$  region, which is expanded in the bottom panel.

the field values at floating profiles. Targeting a posterior on the joint distribution of the floating profile locations and the field values at those locations would be challenging for variational inference due to complex co-dependence. By contrast, the inducing point locations are fixed.

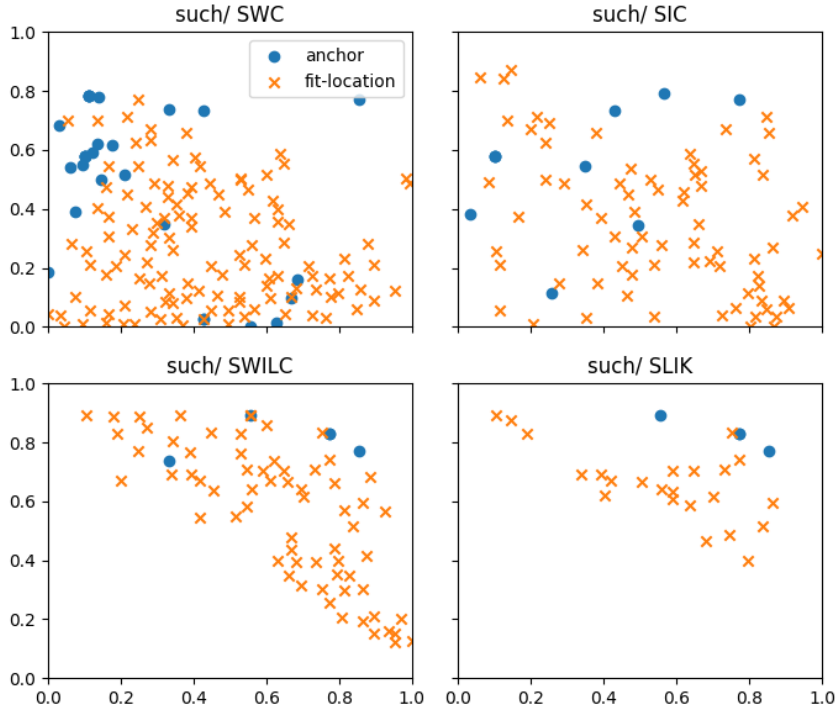


Figure 2: Linguistic Profile locations for four coarsened forms  $\langle \text{SWC} \rangle$ ,  $\langle \text{SIC} \rangle$ ,  $\langle \text{SWILC} \rangle$  and  $\langle \text{SLIK} \rangle$  of the item  $\{ \text{SUCH} \}$ . These coarsened forms correspond to groups of forms in the uncoarsened data, so for example the form  $\langle \text{SUCH} \rangle$  itself is coarsened to the group of  $\langle \text{SWC} \rangle$ . Anchor profiles are marked with blue circles, while floating profiles locations produced by the fit-technique are shown in orange.

3.2. *Semi-Modular Inference.* Cut models (Liu, Bayarri and Berger, 2009; Plummer, 2015) and Semi-Modular Inference (SMI) (Carmona and Nicholls, 2020, 2022) are forms of Bayesian Multiple Imputation that are useful in settings where some of the priors or likelihoods of the generative model for the data are misspecified. The idea is to break the model up into “good” modules (thought to be well-specified) and “bad” (mis-specified) modules. These methods are natural when there are several datasets in the analysis, each with their own observation model. In that setting one module may be associated with each dataset. Each dataset defines a posterior distribution for the variables appearing in the observation model for that dataset. This definition of a “module” has been formalised in Liu and Goudie (2022b).

Consider for example a model with dependence structure illustrated in fig. 3. The modules are  $\{Y, \psi, \theta\}$  and  $\{Z, \psi\}$ . The two posteriors are respectively  $p(\psi|Z)$  and  $p(\theta, \psi|Y)$ . Suppose the  $Z$ -module is trusted and the  $Y$ -module is not.

3.2.1. *Cut-Model inference.* In Cut model inference, parameters shared between good and bad modules are “imputed” in a first stage analysis using only the information in the good module. In our example the Cut-posterior for  $\psi$  is just  $p(\psi|Z)$ . Parameters in the bad modules are then “analysed” in a second analysis conditioned on the imputed parameters from the first stage. The idea is to stop misspecification in the bad module biasing the posterior for parameters it shares with the good module. In the example

above the joint Cut posterior for  $\psi, \theta$  is

$$(1) \quad p_{cut}(\psi, \theta | Z, Y) = p(\psi | Z) p(\theta | \psi, Y) \\ \propto p(Z | \psi) p(\psi) \times p(Y | \psi, \theta) \frac{p(\theta | \psi)}{p(Y | \psi)}.$$

This is “multiple imputation” because the imputed parameters  $\psi$  have a posterior distribution from the first stage, and the second stage conditions on these random variables. Yu, Nott and Smith (2021) show that the Cut-posterior is the joint distribution of  $\psi, \theta$  minimising the KL-divergence to the Bayes posterior

$$p(\psi, \theta | Z, Y) = p(\psi | Z, Y) p(\theta | \psi, Y) \\ \propto p(Z | \psi) p(\psi) \times p(Y | \psi, \theta) p(\theta | \psi)$$

over all distributions  $q(\psi, \theta)$  with  $\psi$ -marginal  $q(\psi) = p(\psi | Z)$ . The Cut-posterior is not a Bayesian belief update which uses the likelihood as a utility and does not have frequentist coverage of the pseudo-true parameter asymptotically (Pompe and Jacob, 2021).

However, Carmona and Nicholls (2020) show that the Cut-model belief update uses a different utility and is coherent in the sense of Bissiri, Holmes and Walker (2016), and Nicholls et al. (2022) shows that the posterior is valid for this utility.

**3.2.2. Semi-Modular Inference.** The setup in SMI is similar. However, in SMI some information from the misspecified module is used in the imputation stage. The idea is to allow the mis-specified module to bias the posterior for shared parameters in order to reduce their variance. This trade off is modulated by an *influence parameter*  $\eta$ . The posterior used for imputation of the shared parameter  $\psi$  is the “power posterior” (Friel and Pettitt, 2008),

$$(2) \quad p_{pow, \eta}(\psi, \tilde{\theta} | Z, Y) \propto p(Z | \psi) p(Y | \psi, \tilde{\theta})^\eta p(\tilde{\theta}, \psi).$$

An auxiliary “copy” of the  $\theta$  parameter is needed in the imputation stage in order to access information from the likelihood  $p(Y | \psi, \tilde{\theta})$ . In the analysis stage we condition on the marginal random variable  $\psi \sim p_{pow, \eta}(\psi | Z, Y)$ , so the full joint Semi-Modular Posterior (SMP) can be taken to be

$$(3) \quad p_{smi, \eta}(\psi, \theta, \tilde{\theta} | Z, Y) = p_{pow, \eta}(\psi, \tilde{\theta} | Z, Y) p(\theta | \psi, Y).$$

This reduces to  $p_{cut}$  when  $\eta = 0$  and gives standard Bayesian inference when  $\eta = 1$  so the SMP uses the power posterior to give a sequence of distributions interpolating Bayes and Cut (Carmona and Nicholls, 2020). Recent variants of SMI suggest alternative interpolating sequences of distributions (Liu and Goudie, 2021; Chakraborty et al., 2022; Nicholls et al., 2022) within the same framework.

**3.2.3. Targeting the Semi-Modular Posterior.** Targeting the SMP with MCMC is not straightforward due to the marginal factor  $p(Y | \psi)$  in eq. (1) and eq. (3). A form of nested MCMC (Plummer, 2015) is straightforward and adequate for many simple problems (Carmona and Nicholls, 2020). For any given value of the influence parameter  $\eta$ , we first obtain  $T_1$  samples  $(\psi^{(t)}, \tilde{\theta}^{(t)})_{t=1}^{T_1}$  from the power posterior  $p_{pow, \eta}(\psi, \tilde{\theta} | Z, Y)$  using MCMC. In the second stage, for each sample  $\psi^{(t)}$ , we run a sub-chain  $(\theta^{(t, \tau)})_{\tau=1}^{T_2}$  targeting  $p(\theta | \psi^{(t)}, Y)$  to equilibrium, preserving only the last sample  $\theta^{(t)} = \theta^{(t, T_2)}$  of each sub-chain. The samples returned by the two-stage sampler are  $(\psi^{(t)}, \theta^{(t)}, \tilde{\theta}^{(t)})_{t=1}^{T_1}$ . This can be done using standard MCMC algorithms. Asymptotically in  $T_1$  and  $T_2$ , the triples  $(\psi^{(t)}, \tilde{\theta}^{(t)}, \theta^{(t)}) \sim p_{smi, \eta}$  have the desired distribution. We found this worked well on our

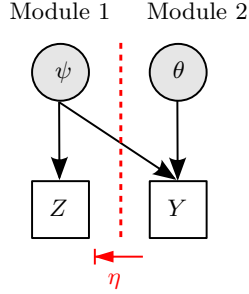


Figure 3: A Cut-model with two modules. The first module has parameter  $\psi$  and data  $Z$ , while the second is defined conditionally upon  $\psi$ , with parameter  $\theta$  and data  $Y$ .

problem if the number of items and floats in the data was small (of order ten items and ten floats), but too slow on the full dataset. This motivates our use of Variational SMI. Besides this nested MCMC, other Monte-Carlo methods (Jacob, O’Leary and Atchadé, 2020; Liu and Goudie, 2022a) have been given for the Cut-model. These could be used for SMI. However, although they remove the double asymptotics and provide better guarantees on sample quality, they are in general slower than Nested MCMC and we have not explored them here. Some further implementation detail is given in section 6.2.

In Variational SMI, the aim is to find a distribution  $q_\lambda(\psi, \theta, \hat{\theta})$  that approximates the SMP in eq. (3). Straightforward minimisation of the KL-divergence loss to the SMP over a variational family  $q_\lambda$  is neither feasible (on account of the intractable marginal  $p(Y|\psi)$  factor) nor in fact desirable (as we would lose control of the influence of bad modules on parameters shared with good modules). Recently, Yu, Nott and Smith (2021) and Carmona and Nicholls (2022) gave a variational loss for approximation of Cut-models and the Semi-Modular Posterior that preserves control of information flow in the approximating posterior and is feasible to fit using Stochastic Gradient Descent (SGD). We explain how this applies in our setting in section 6.3.

**4. Model.** In this section we give our statistical model for the LALME data described in section 2.

4.1. *Observation model.* Imagine a medieval scribe writing sample text  $p \in \mathcal{P}$ . They use item  $i \in \mathcal{I}$  a certain number of times,  $z_{p,i}$ . Each time they use item  $i$  they choose a form  $f \in \mathcal{F}_i$  for the item to take (informally, each time they write a word they choose a spelling). The probability  $\phi_{i,f}(x_p)$  for them to choose any particular form depends on their location  $x_p$  (recall, location here is the source of the scribe’s dialect, for example, their place of schooling; for anchor texts this is taken to be the place at which the text was created, in the absence of evidence to the contrary). For  $x \in \mathcal{X}$  let

$$\phi_i(x) = (\phi_{i,1}(x), \dots, \phi_{i,F_i}(x))$$

give the vector of form-selection probabilities for item  $i$  at location  $x$ , with  $\sum_{f=1}^{F_i} \phi_{i,f}(x) = 1$ . Suppose that, by the end of the text they use form  $f \in \mathcal{F}_i$  in all  $z_{p,i,f}$  times so that  $z_{p,i} = \sum_{f \in \mathcal{F}_i} z_{p,i,f}$ .

Some items represent words which express ideas which come up more often in texts. For  $i \in \mathcal{I}$  let  $\mu_i$  give the mean number of times item  $i$  appears in any given text, let  $\mu = (\mu_i)_{i \in \mathcal{I}}$  and

$$(z_{p,i} \mid \mu_i) \sim \text{Poisson}(\mu_i) \quad \text{iid for } p \in \mathcal{P}.$$

This does not depend on location  $x_p$  as the selection of items (which depends on the topic of the text) is assumed to be location-independent. Let  $\mathbf{Z}_{p,i} = (z_{p,i,1}, \dots, z_{p,i,F_i})$ . If forms are chosen independently then

$$(\mathbf{Z}_{p,i} \mid z_{p,i}, \phi_i(x_p)) \sim \text{Multinomial}(\phi_i(x_p), z_{p,i}) \quad \text{iid for } p \in \mathcal{P} \text{ and } i \in \mathcal{I}$$

so the joint distribution for the count data  $Z_{\mathcal{P}} = (\mathbf{Z}_{p,i})_{p \in \mathcal{P}}^{i \in \mathcal{I}}$  is

$$p(Z_{\mathcal{P}} \mid \mu, \Phi(X_{\mathcal{P}})) = \prod_{p \in \mathcal{P}} \prod_{i \in \mathcal{I}} \prod_{f \in \mathcal{F}_i} \frac{e^{-\mu_i \phi_{i,f}(x_p)} (\mu_i \phi_{i,f}(x_p))^{z_{p,i,f}}}{z_{p,i,f}!}$$

where  $\Phi(X_{\mathcal{P}}) = (\phi_i(x_p))_{p \in \mathcal{P}}^{i \in \mathcal{I}}$  collects the form frequencies for all items at all profile locations. Here  $\Phi(X_{\mathcal{P}}) \in [0, 1]^{d_{\Phi}}$  is a  $d_{\Phi} = \sum_{i \in \mathcal{I}} F_i$  dimensional vector.

We now give the observation model for the observed presence/absence data  $y_{p,i,f} \in \{0, 1\}$ ,  $p \in \mathcal{P}$ ,  $i \in \mathcal{I}$ ,  $f \in \mathcal{F}_i$ . We allow zero inflation in these records in order to account for missing items, so we do not simply set  $y_{p,i,f} = \mathbb{I}(z_{p,i,f} > 0)$ . Also, texts have topics, and this may preclude a given item appearing. Some ‘‘specialist’’ items may appear frequently when on-topic and otherwise be absent. Let  $\zeta = (\zeta_i)_{i \in \mathcal{I}}$ ,  $\zeta_i \in [0, 1]$  give the zeroing-probability parameters which vary from item to item. With these

$$p(y_{p,i,f} = 0 \mid \mu_i, \zeta_i, \phi_{i,f}(x_p)) = \zeta_i + (1 - \zeta_i) e^{-\mu_i \phi_{i,f}(x_p)},$$

and so the joint likelihood for the binary data is

$$(4) \quad p(Y_{\mathcal{P}} \mid \mu, \zeta, \Phi(X_{\mathcal{P}})) = \prod_{p \in \mathcal{P}} \prod_{i \in \mathcal{I}} \prod_{f \in \mathcal{F}_i} p(y_{p,i,f} \mid \mu_i, \zeta_i, \phi_{i,f}(x_p)) \\ = \prod_{p \in \mathcal{P}} \prod_{i \in \mathcal{I}} \prod_{f \in \mathcal{F}_i} \zeta_i (1 - y_{p,i,f}) + (1 - \zeta_i) \beta_{i,f}(x_p)$$

where  $\beta_{i,f}(x_p) = (1 - e^{-\mu_i \phi_{i,f}(x_p)})^{y_{p,i,f}} (e^{-\mu_i \phi_{i,f}(x_p)})^{1 - y_{p,i,f}}$ . Haines (2016) includes an additional outlier model which identifies some items within some profiles as unreliable.

*4.2. Prior distributions.* The parameters in the observational model in eq. (4) are the item intensities  $\mu \in [0, \infty)^I$ , the zero-inflation parameters  $\zeta \in [0, 1]^I$  and the form-probability fields  $\Phi(X_{\mathcal{P}})$  at all locations  $X_{\mathcal{P}} = (X_A, X_{\bar{A}})$ . The unknown locations of floating profiles,  $X_{\bar{A}} = (X_i)_{i \in \bar{A}}$ , are also parameters of the model. In the following we assume an independent prior for each of these quantities.

We define the prior for the item intensity parameters  $\mu$  following prior elicitation from an Atlas author. We use Gamma distributions with common shape and rate parameters  $a = b = 3$  so

$$p(\mu) = \prod_{i=1}^I \text{Gamma}(\mu_i; a, b).$$

For the zero-inflation probabilities we use uniform priors so that

$$p(\zeta) = \prod_{i \in \mathcal{I}} \mathbb{I}(0 \leq \zeta_i \leq 1).$$

This reflects the fact that we expect zero inflation events to be rather common. For the missing locations  $p(X_{\bar{A}})$ , we assume independent uniform priors over the rectangular region of interest, rescaling easting  $\times$  northing into  $\mathcal{X} = [0, 1] \times [0, 0.9]$  and yielding

$$p(X_{\bar{A}}) \propto \prod_{p=N+1}^{N+M} \mathbb{I}(x_p \in \mathcal{X}).$$

It may be possible to elicit more informative priors for  $x_p$ ,  $p \in \bar{A}$ , for example, proportional to population density if historical population density maps were available.

The latent linguistic fields giving form-usage probabilities have one field for each form of each item, in total  $d_\phi = \sum_{i=1}^I F_i$  fields. Denote the collection of all *probability fields* as  $\Phi = \{\phi_{i,f}(x)\}_{i \in \mathcal{I}, f \in \mathcal{F}_i, x \in \mathcal{X}}$ . In building a model for these fields, three considerations apply: first, at any given location  $x \in \mathcal{X}$ , the fields associated with item  $i$  must sum to one,  $\sum_{f \in \mathcal{F}_i} \phi_{i,f}(x) = 1$ ; second, field values at nearby locations should be correlated; and third, fields of different items should be correlated by substructure in the population of speakers.

In order to satisfy the location-additivity requirement, we parameterise the probability fields  $\phi_{i,f}(x)$ ,  $i \in \mathcal{I}, f \in \mathcal{F}_i, x \in \mathcal{X}$  using a *softmax* transformation of *intensity fields*  $\gamma_{i,f}(x) \in \mathbb{R}$  such that

$$\phi_{i,f}(x) = \frac{\exp(\gamma_{i,f}(x))}{\sum_{f' \in \mathcal{F}_i} \exp(\gamma_{i,f'}(x))}.$$

The second and third requirements are satisfied by using Gaussian Process (GP) priors (Rasmussen and Williams, 2005) for the form intensity fields. Specifically, we use a Linear Model of Coregionalization (LMC) (Journel and Huijbregts, 1978; Álvarez, Rosasco and Lawrence, 2012) to induce correlation across locations and between items. Let  $\mathcal{B} = \{1, \dots, B\}$  and  $\Gamma = \{\gamma_b(x)\}_{b \in \mathcal{B}, x \in \mathcal{X}}$  denote a collection of  $B$  independent GP *basis fields* with common kernel,

$$\gamma_b(x) \sim GP(0, k(\cdot, \cdot)), \quad b \in \mathcal{B},$$

and define the intensity fields as a linear combination these basis GPs by using a set of mixing weights and offsets,

$$(5) \quad \gamma_{i,f}(x) = a_{i,f} + \sum_{b=1}^B \gamma_b(x) w_{i,f,b}.$$

The use of LMC in a GP setting seems to be the key to the significant performance-improvement we see over Haines (2016), who used an independent Markov Random Field with a local L1 smoothness penalty for each field  $\phi_{i,f}(x)$ . Haines (2016) saw a complete collapse in reconstruction accuracy as items and floating profiles are added to a Bayesian analysis. The present model, in which  $B$  need not grow indefinitely with increasing  $I$ , avoids this collapse.

Let  $a = (a_{i,f})_{i \in \mathcal{I}, f \in \mathcal{F}_i}$  and  $W = (w_{i,f,b})_{i \in \mathcal{I}, f \in \mathcal{F}_i, b \in \mathcal{B}}$ . We set independent Laplace priors for the weights to induce sparsity, and Gaussian priors for the offsets

$$p(a) = \prod_{i=1}^I \prod_{f=2}^{F_i} p(a_{i,f}) \quad \text{with } a_{i,f} \sim \text{Normal}(0, \sigma_a)$$

$$p(W) = \prod_{b=1}^B \prod_{i=1}^I \prod_{f=1}^{F_i} p(w_{i,f,b}) \quad \text{with } w_{i,f,b} \sim \text{Laplace}(0, \sigma_w)$$

In order to avoid identifiability issues, we set the offset for the first form of each item  $a_{i,1}$  to 0. In our experiments, we use a Squared Exponential Covariance for the Kernel of the basis GPs. The kernel hyper-parameters were set via Hyper-Parameter Optimisation (HPO) (described in section 6.4).

The Linear Model of Coregionalization not only induces prior correlation between items, but also reduces the model dimension significantly. We only need  $B$  GPs priors, instead of the  $\sum_{i=1}^I F_i - I$  priors required if we set independent priors for forms within

an item. In our experiments, we find that a small number of basis fields (around  $B \simeq 10$ ) are enough to capture the geographical structure of the linguistic fields (see section 7). This is orders of magnitude smaller than directly setting a prior on the hundreds of intensity fields. However, it is also desirable from a prior elicitation perspective: underlying population structure could correlate the frequencies of different forms across space; basis fields express spatial co-dependence in the variation of the frequencies of many forms across space in a parsimonious way.

Let  $\Gamma_b(X_{\mathcal{P}}) = (\gamma_b(x_p))_{p \in \mathcal{P}}$  be the vector of values taken by one basis field  $b \in \mathcal{B}$  at all profile locations, so that  $\Gamma_b(X_{\mathcal{P}}) \in \mathbb{R}^P$  and let  $\Gamma(X_{\mathcal{P}}) = (\Gamma_b(X_{\mathcal{P}}))_{b \in \mathcal{B}}$  be the vector of all basis-field values at all profile locations, with  $\Gamma(X_{\mathcal{P}}) \in \mathbb{R}^{B \times P}$ . In this construction, the prior for the probability fields  $\Phi(X_{\mathcal{P}})$  at profile locations is determined by the GPs prior of the basis fields and the mixing coefficients,  $p(\Gamma(X_{\mathcal{P}}), a, W)$ .

**4.3. Exact Joint Probabilistic Model.** In this section we set out the joint model for the parameters and data, collecting all the elements described above into a joint probabilistic model. In the next section we will give an approximation to this distribution which is needed for tractability.

Given the deterministic relation between the probability fields  $\Phi$  and their constituents  $(\Gamma, a, W)$  under the LMC, we rewrite the observational model from eq. (4) as

$$p(Y_{\mathcal{P}} | \mu, \zeta, \Phi(X_{\mathcal{P}})) \equiv p(Y_{\mathcal{P}} | \mu, \zeta, a, W, \Gamma(X_{\mathcal{P}})).$$

Let  $\Gamma(X_A) = (\Gamma_b(X_A))_{b \in \mathcal{B}}$  and  $\Gamma(X_{\bar{A}}) = (\Gamma_b(X_{\bar{A}}))_{b \in \mathcal{B}}$  give the vectors of basis fields at anchors and floats respectively. The exact joint probabilistic model of data and parameters is

$$(6) \quad \begin{aligned} p(Y_{\mathcal{P}}, \mu, \zeta, a, W, \Gamma(X_{\mathcal{P}}), X_{\bar{A}}) &= p(Y_A | \mu, \zeta, a, W, \Gamma(X_A)) p(Y_{\bar{A}} | \mu, \zeta, a, W, \Gamma(X_{\bar{A}})) \\ &\times p(\Gamma(X_A), \Gamma(X_{\bar{A}}) | X_{\bar{A}}) \\ &\times p(X_{\bar{A}}) p(\mu, \zeta, a, W) \end{aligned}$$

Exact inference on this probabilistic model becomes computationally infeasible with a large number of profiles in the data. The joint distribution of the values  $\Gamma_b(X_{\mathcal{P}})$  taken by one basis field  $b \in \mathcal{B}$  at all profile locations, is a multivariate Gaussian of dimension  $P = N + M$ , with zero mean and covariance matrix  $K_P = (k(x_i, x_j))_{i, j \in \mathcal{P}}$ ,

$$\Gamma_b(X_{\mathcal{P}}) \sim \text{Normal}(0, K_P),$$

and we need to compute the inverse of  $K_P$  many times over when targeting the posterior. This won't scale to the full LALME dataset, which contains thousands of profiles  $P$ .

**4.4. Sparsity in Latent Fields via Inducing Points.** In order to overcome the scalability challenge on the number of profiles, we introduce a sparse approximation to the joint distribution in eq. (6) via inducing points (Titsias, 2009; Bonilla, Krauth and Dezfouli, 2019; Quiñonero-Candela and Rasmussen, 2005). Inducing values augment the prior specification and serve as *global parameters* that are particularly convenient in SVI (Hensman, Fusi and Lawrence, 2013; Hensman, Matthews and Ghahramani, 2015). There are two steps to the approximation: we indicate the exact joint model by  $p(\cdot)$  in eq. (6) and the first and second stage of the approximation by  $p^{(1)}$  and  $p^{(2)}$  in eq. (9) and eq. (12) below.

Consider a set of  $U$  *inducing points*,  $X_{\mathcal{U}} = (x_u)_{u \in \mathcal{U}}$ ,  $\mathcal{U} = \{1, \dots, U\}$  and for  $b \in \mathcal{B}$  let  $\Gamma_b(X_{\mathcal{U}}) = (\gamma_b(x_u))_{u \in \mathcal{U}}$ . Here  $\Gamma_b(X_{\mathcal{U}})$  is a multivariate Gaussian random variable of dimension  $U$ , with zero mean and covariance matrix  $K_U = (k(x_i, x_j))_{i, j \in \mathcal{U}}$ ,

$$\Gamma_b(X_{\mathcal{U}}) \sim \text{Normal}(0, K_U).$$

We call  $\Gamma_b(X_U)$  the *inducing values* of basis field  $b$ . Let  $\Gamma(X_U) = (\Gamma_b(X_U))_{b \in \mathcal{B}}$  be the vector of all inducing values for all basis fields.

In the sparse approximation the prior distribution for the basis GPs at profiles,  $p(\Gamma(X_{\mathcal{P}}) = (\Gamma(X_A), \Gamma(X_{\bar{A}})))$ , and inducing locations,  $\Gamma(X_U)$ , is approximated by assuming conditional independence between fields values,  $\Gamma(X_A)$  and  $\Gamma(X_{\bar{A}})$ , at anchor and floating profiles given the inducing values, that is

$$(7) \quad \begin{aligned} p(\Gamma(X_{\mathcal{P}}), \Gamma(X_U) \mid X_{\bar{A}}) &= p(\Gamma(X_A), \Gamma(X_{\bar{A}}) \mid \Gamma(X_U), X_{\bar{A}}) p(\Gamma(X_U)) \\ &\approx p(\Gamma(X_A) \mid \Gamma(X_U)) p(\Gamma(X_{\bar{A}}) \mid \Gamma(X_U), X_{\bar{A}}) p(\Gamma(X_U)). \end{aligned}$$

This is likely to be a better approximation than is often seen in inducing point approximations, as it retains correlation within the anchor group and within the group of floats. One popular setup (Hensman, Matthews and Ghahramani, 2015) would take all fields at all profile locations to be jointly independent given the inducing values.

In our experiments, we define a homogeneous square grid of inducing points along the region of interest by dividing in 10 sections vertically and horizontally, for a total of 121 inducing points. The space between inducing points corresponds to approximately 20 km in the map which is somewhat shorter than the scale of variation we recover (see fig. 15). Our approximation will be good if the inter-point spacing of inducing points is smaller than the length scale for variation in the basis fields.

We now specify the factors appearing in eq. (7). In fig. 4 we display a graphical representation of the model we are describing. The joint distribution of the values of basis field  $b$  at anchor locations conditioned on the values taken by field  $b$  at inducing points is

$$(8) \quad (\Gamma_b(X_A) \mid \Gamma_b(X_U)) \sim \text{Normal}(K_{A,U} K_U^{-1} \Gamma_b(X_U), K_A - K_{A,U} K_U^{-1} K_{A,U}^t),$$

where  $K_A = (k(x_p, x_q))_{p,q \in A}$  is the covariance matrix between anchor locations, and  $K_{A,U} = (k(x_i, x_j))_{i \in A, j \in U}$  is the cross-covariance matrix between anchor profiles and inducing locations. The conditional distribution  $(\Gamma_b(X_{\bar{A}}) \mid \Gamma_b(X_U), X_{\bar{A}})$  of the basis field values at floating profiles locations  $X_{\bar{A}}$  is given by eq. (8) with  $A \rightarrow \bar{A}$ .

By the prior independence of basis fields we have  $p(\Gamma(X_U)) = \prod_{b=1}^B p(\Gamma_b(X_U))$ , a product of multivariate Gaussians of dimension  $U$ . Similarly,

$$p(\Gamma(X_A) \mid \Gamma(X_U)) = \prod_{b=1}^B p(\Gamma_b(X_A) \mid \Gamma_b(X_U)),$$

a product of multivariate Gaussians of dimension  $N$ . For the floating profiles,

$$p(\Gamma(X_{\bar{A}}) \mid \Gamma(X_U), X_{\bar{A}}) = \prod_{b=1}^B p(\Gamma_b(X_{\bar{A}}) \mid \Gamma_b(X_U), X_{\bar{A}}),$$

the factors each have dimension  $M$ . The approximate joint density after this first factorising approximation is

$$(9) \quad \begin{aligned} p^{(1)}(Y_{\mathcal{P}}, \mu, \zeta, a, W, \Gamma(X_U), \Gamma(X_{\mathcal{P}}), X_{\bar{A}}) &= p(Y_A \mid \mu, \zeta, a, W, \Gamma(X_U)) p(Y_{\bar{A}} \mid \mu, \zeta, a, W, \Gamma(X_U)) \\ &\times p(\Gamma(X_A) \mid \Gamma(X_U)) p(\Gamma(X_{\bar{A}}) \mid \Gamma(X_U), X_{\bar{A}}) \\ &\times p(X_{\bar{A}}) p(\Gamma(X_U)) p(\mu, \zeta, a, W) \end{aligned}$$

We make an additional approximation in order to compute the joint log-probability: we make an approximate integration over the fields at profile locations, following Hensman, Matthews and Ghahramani (2015),

$$\log p(Y_A \mid \mu, \zeta, a, W, \Gamma(X_U)) = \log \left[ \mathbb{E}_{p(\Gamma(X_A) \mid \Gamma(X_U))} p(Y_A \mid \mu, \zeta, a, W, \Gamma(X_A)) \right]$$

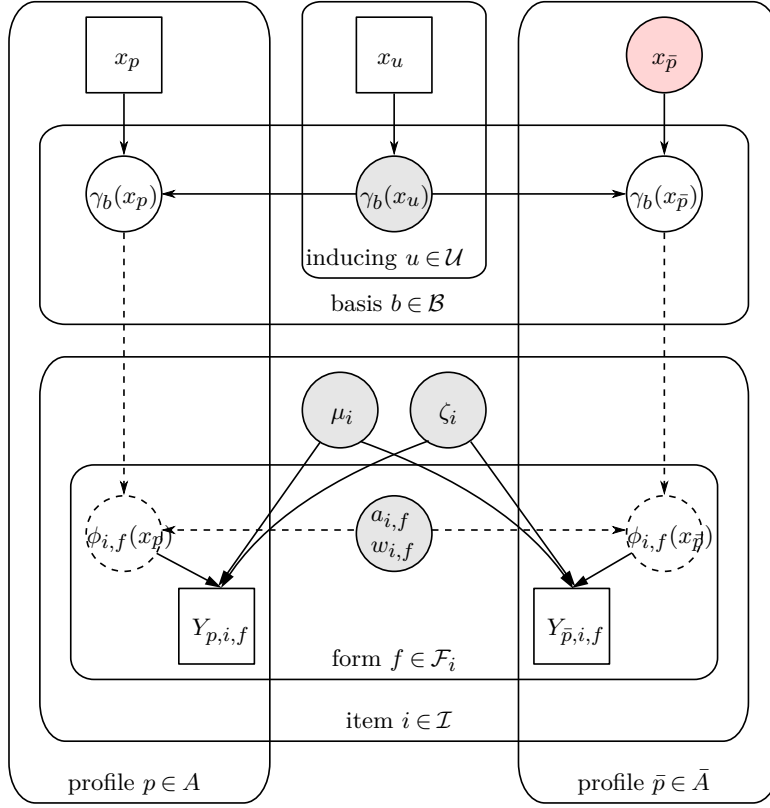


Figure 4: Probabilistic Graphical Model for the Linguistic Data. Squares represent observed data, circles represent model parameters. Global parameters are at the core of the model, colored in grey, and the missing locations colored in red. Probabilistic relationships are represented by solid lines, while dashed lines represent deterministic relations. Plates denote multiplicity along sets.

$$\begin{aligned}
 &\geq \mathbb{E}_{p(\Gamma(X_A)|\Gamma(X_U))} [\log p(Y_A | \mu, \zeta, a, W, \Gamma(X_A))] \\
 (10) \quad &\equiv \log \tilde{p}(Y_A | \mu, \zeta, a, W, \Gamma(X_U))
 \end{aligned}$$

$$\begin{aligned}
 \log p(Y_{\bar{A}} | \mu, \zeta, a, W, \Gamma(X_U), X_{\bar{A}}) &\geq \mathbb{E}_{p(\Gamma(X_{\bar{A}})|\Gamma(X_U), X_{\bar{A}})} [\log p(Y_{\bar{A}} | \mu, \zeta, a, W, \Gamma(X_{\bar{A}}), X_{\bar{A}})] \\
 (11) \quad &\equiv \log \tilde{p}(Y_{\bar{A}} | \mu, \zeta, a, W, \Gamma(X_U), X_{\bar{A}}).
 \end{aligned}$$

We approximate the likelihoods on the left with the lower bounds on the right, so that the final approximated joint probability distribution is

$$\begin{aligned}
 (12) \quad p^{(2)}(Y_{\mathcal{P}}, \mu, \zeta, a, W, \Gamma(X_U), X_{\bar{A}}) &= \tilde{p}(Y_A | \mu, \zeta, a, W, \Gamma(X_U)) \\
 &\quad \times \tilde{p}(Y_{\bar{A}} | \mu, \zeta, a, W, \Gamma(X_U), X_{\bar{A}}) \\
 &\quad \times p(\mu, \zeta, a, W, \Gamma(X_U), X_{\bar{A}}).
 \end{aligned}$$

Whenever we need to evaluate eq. (10) or eq. (11) we estimate their values by drawing joint samples  $\Gamma(X_A) \sim p(\cdot | \Gamma(X_U))$  and  $\Gamma(X_{\bar{A}}) \sim p(\cdot | \Gamma(X_U), X_{\bar{A}})$  and averaging. We found by experiment that 100 samples was sufficient for stable downstream inference.

**5. Semi-Modular Inference for the LALME model.** In the context of a different model for the spatial fields, Haines (2016) observes that jointly inferring the spatial fields and the locations of all floating profiles yields poor results, with floating profiles often clustering together at the borders of the region. Model error in the field-prior is amplified by feedback from floating profiles and can dominate information from anchors. This suggested a *Cut Posterior* setup (Haines, 2016, p. 125) in which the posterior distribution of the fields was estimated using the anchor profiles alone, and then the posterior distribution of the floating-profile locations was obtained by averaging over the field posteriors. This two-stage approach, which eliminates information flow from the floating profiles to the spatial fields, out-performed Bayesian inference.

Reducing feedback between *modules* is an effective way to alleviate model contamination (Liu, Bayarri and Berger, 2009; Jacob et al., 2017). A graphical representation of this Cut in the LALME model is displayed in fig. 5. If we group together elements of the probabilistic model in fig. 5 we get exactly the two-module model in fig. 3,

$$(13) \quad \begin{aligned} Z &\equiv Y_A, & Y &\equiv Y_{\bar{A}}, \\ \theta &\equiv X_{\bar{A}}, & \psi &\equiv (\mu, \zeta, a, W, \Gamma(X_U)). \end{aligned}$$

We begin by giving the cut posterior and then extend the analysis to give the SMP. Using our model specification, the cut posterior eliminating the feedback from floating profiles into linguistic fields is given by

$$(14) \quad \begin{aligned} p_{cut}(\mu, \zeta, a, W, \Gamma(X_U), X_{\bar{A}} | Y_{\mathcal{P}}) &= p(\mu, \zeta, a, W, \Gamma(X_U) | Y_A) \\ &\quad \times p(X_{\bar{A}} | \mu, \zeta, a, W, \Gamma(X_U), Y_{\bar{A}}), \end{aligned}$$

which, when written in the notation of eq. (13), is identical to eq. (1). The approximations given in eq. (10) and eq. (11) are needed in both stages, so that

$$\begin{aligned} p(\mu, \zeta, a, W, \Gamma(X_U) | Y_A) &\propto \tilde{p}(Y_A | \mu, \zeta, a, W, \Gamma(X_U)) p(\mu, \zeta, a, W, \Gamma(X_U)), \\ p(X_{\bar{A}} | \mu, \zeta, a, W, \Gamma(X_U), Y_{\bar{A}}) &\propto \tilde{p}(Y_{\bar{A}} | \mu, \zeta, a, W, \Gamma(X_U), X_{\bar{A}}) p(X_{\bar{A}}), \end{aligned}$$

where we omitted a factor  $p(Y_{\bar{A}} | \mu, \zeta, a, W, \Gamma(X_U))$  in the second denominator. This is constant for any fixed set of conditioning variables, and corresponds to  $p(Y|\psi)$  in eq. (1). This wont play a role in our MCMC or SVI due to the two-stage structure they share.

We now extend the modularized analysis of Haines (2016) to Semi-Modular Inference (SMI) (Carmona and Nicholls, 2020). In order to define the Semi-Modular Posterior in our setting, we simply drop the objects defined in eq. (13) into the power posterior eq. (2) and SMI posterior eq. (3). We define a scalar influence parameter  $\eta \in [0, 1]$  which enters as a power on the likelihood factor for floats and define the *powered* joint distribution

$$(15) \quad \begin{aligned} p_{pow,\eta}(\mu, \zeta, a, W, \Gamma(X_U), X_{\bar{A}} | Y_{\mathcal{P}}) &\propto \tilde{p}(Y_A | \mu, \zeta, a, W, \Gamma(X_U)) \\ &\quad \times \tilde{p}(Y_{\bar{A}} | \mu, \zeta, a, W, \Gamma(X_U), X_{\bar{A}})^\eta \\ &\quad \times p(\mu, \zeta, a, W, \Gamma(X_U)) p(X_{\bar{A}}). \end{aligned}$$

We have replaced exact likelihoods  $p(Y_A | \mu, \zeta, a, W, \Gamma(X_U))$  and  $p(Y_{\bar{A}} | \mu, \zeta, a, W, \Gamma(X_U))$  with the lower bound approximations given in eq. (10) and eq. (11). The notation of eq. (13) identifies eq. (15) with eq. (2).

The Semi-Modular Posterior is obtained by using this power-posterior and creating auxiliary copies of selected model parameters, namely  $\tilde{\theta} \equiv \tilde{X}_{\bar{A}}$ . The Semi-Modular Posterior for the LALME model is then

$$(16) \quad \begin{aligned} p_{smi,\eta}(\mu, \zeta, a, W, \Gamma(X_U), X_{\bar{A}}, \tilde{X}_{\bar{A}} | Y_{\mathcal{P}}) &\propto p_{pow,\eta}(\mu, \zeta, a, W, \Gamma(X_U), \tilde{X}_{\bar{A}} | Y_{\mathcal{P}}) \\ &\quad \times p(X_{\bar{A}} | \mu, \zeta, a, W, \Gamma(X_U), Y_{\bar{A}}). \end{aligned}$$

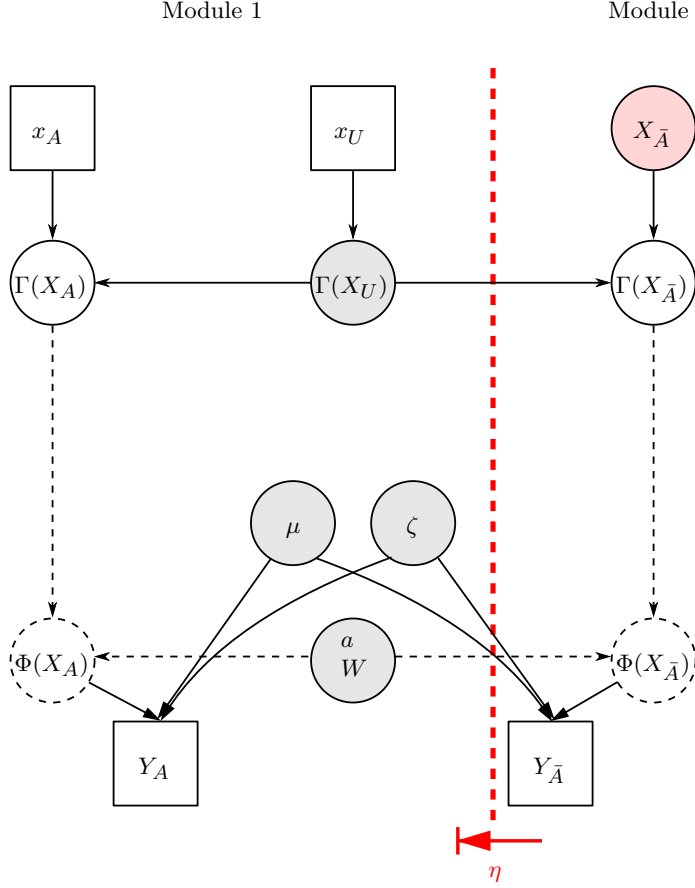


Figure 5: Probabilistic Graphical Model for the Linguistic Data. The plates are omitted for simplicity. Notation is otherwise as fig. 4. The red dashed line indicates the cut. In the cut-posterior, parameters on the left side of the cut are inferred independently of any information from the right side. In SMI, information from the right is downweighted.

In the notation of eq. (13), eq. (16) is

$$(17) \quad p_{\text{smi},\eta}(\psi, \theta, \tilde{\theta} | Y_A, Y_{\bar{A}}) = p_{\text{pow},\eta}(\psi, \tilde{\theta} | Y_A, Y_{\bar{A}}) p(\theta | \psi, Y_{\bar{A}})$$

and so we can identify the Semi-Modular Posterior in eq. (16) for the model in fig. 5 with the Semi-Modular Posterior in eq. (3) for the model in fig. 3. The Semi-Modular Posterior in eq. (16) interpolates between the cut posterior in eq. (14) and the (approximate) Bayes posterior in eq. (12).

5.1. *Choosing the rate of influence.* The selection of the influence parameter  $\eta$  will depend on the goals of inference. We define a *loss function*  $V : [0, 1] \rightarrow \mathbb{R}$  that measures success in the inference and chose the influence parameter that minimises this loss,

$$\eta^* = \arg \min_{\eta} V(\eta).$$

The SMP distribution corresponding to  $\eta^*$  is used for downstream analyses.

In the context of the present problem, the loss function should measure the accuracy of our  $X_{\bar{A}}$ -estimation as a function of the influence  $\eta$  of the float data  $Y_{\bar{A}}$ . We do not of

course know the true float locations,  $X_{\bar{A}}^*$  say, but we do have an obvious proxy in the anchor locations  $X_A$ . We therefore take the Posterior Mean Squared Error for predicting anchor locations as our loss. We treat  $K = 20$  anchors as floats and adjust  $\eta$  so that the posterior for their locations are concentrated on their true locations using the posterior MSE as a loss encapsulating a penalty for the bias and variance of location estimates.

Let  $\mathcal{K} = \{i_1, \dots, i_K\}$  denote the indices of the ‘‘held out’’ anchors, so that  $\mathcal{K} \subset \mathcal{I}$ , and  $A \setminus \mathcal{K}$  are the indices of the remaining anchors. Relabel the true locations of the held out anchors  $X_{\mathcal{K}}^*$  and let  $X_{\bar{A} \cup \mathcal{K}} \in \mathcal{X}^{M+K}$  denote all the locations we wish to estimate in this cross-validation analysis and let  $\tilde{X}_{\bar{A} \cup \mathcal{K}}$  be a second copy of the same parameters. In this analysis the SMP in eq. (17) is

$$(18) \quad p_{\text{smi},\eta}^{(\text{val})}(\psi, X_{\bar{A} \cup \mathcal{K}}, \tilde{X}_{\bar{A} \cup \mathcal{K}} | Y_{\mathcal{P}}) = p_{\text{pow},\eta}(\psi, \tilde{X}_{\bar{A} \cup \mathcal{K}} | Y_{A \setminus \mathcal{K}}, Y_{\bar{A} \cup \mathcal{K}}) p(X_{\bar{A} \cup \mathcal{K}} | \psi, Y_{\bar{A} \cup \mathcal{K}}),$$

and we have the standard SMI setup of eq. (3) with

$$(19) \quad \begin{aligned} Z &\equiv Y_{A \setminus \mathcal{K}}, & Y &\equiv Y_{\bar{A} \cup \mathcal{K}}, \\ \theta &\equiv X_{\bar{A} \cup \mathcal{K}}, & \psi &\equiv (\mu, \zeta, a, W, \Gamma(X_{\mathcal{U}})). \end{aligned}$$

Our loss function is then,

$$(20) \quad V(\eta) = K^{-1} \sum_{p \in \mathcal{K}} \mathbb{E}_{p_{\text{smi},\eta}^{(\text{val})}} \left[ \|x_p - X_p^*\|^2 \right],$$

where  $\|x_p - X_p^*\|$  is Euclidean norm and for  $p \in \mathcal{K}$ ,  $x_p$  and  $X_p^*$  are the posterior and known true profile locations for the  $K = 20$  held out anchors.

A design like this is discussed in Mao, Martin and Reich (2022). If, for example, the pairs  $(x_p, y_p)_{p \in \mathcal{P}}$  were exchangeable (so  $x_p$ ,  $p \in \bar{A}$  is unknown, but the missingness is random) then the distribution of the ‘‘held out’’ anchor loss  $\|x_p - X_p^*\|^2$ ,  $p \in \mathcal{K}$  at any given  $\eta$  would be the same as the ‘‘ideal’’ loss  $\|x_p - X_p^*\|^2$  for  $p \in \bar{A}$  a float, and hence a good proxy for the ideal target loss. Exchangeability does not hold in our spatial setting so this idealised. A form of local-exchangeability developed by Mao, Martin and Reich (2022) may hold. However, we have not explored this.

## 6. Implementation details.

6.1. *Data settings.* Recall our description of the LALME data from section 2. The observations come from a rectangular region spanning 200 km east-west and 180 km north-south. The region contains  $N = 120$  anchor profiles and  $M = 247$  floating profiles. In these profiles we have in all  $I = 71$  items producing  $\sum_{i=1}^I f_i = 741$  distinct forms. We consider four datasets in our experiments: the *full dataset* containing all data in the region, a *validation dataset* obtained from the full dataset by treating twenty anchors as floats, a *medium dataset* with all the floating profiles but just a subset of the items and a *small dataset* with just a subset of floating profiles and items,

*Full dataset:* 367 profiles ( $N = 120, M = 247$ ),  $I = 71$  items,  $\sum_{i=1}^I f_i = 741$  forms,

*Validation dataset:* 367 profiles ( $N = 100, M = 267$ ),  $I = 71$  items,  $\sum_{i=1}^I f_i = 741$  forms,

*Medium dataset:* 367 profiles ( $N = 120, M = 247$ ),  $I = 8$  items,  $\sum_{i=1}^I f_i = 79$  forms,

*Small dataset:* 120 profiles ( $N = 120, M = 10$ ),  $I = 8$  items,  $\sum_{i=1}^I f_i = 79$  forms.

In table 1 we provide a count of the number of parameters required by the LALME

model for the small and full datasets. The small dataset is motivated as a baseline to compare the estimation between MCMC and variational methods. We found it infeasible to use MCMC when the number of floating profiles is at all large, as we could not get convergence in a reasonable time. This is demonstrated using the medium dataset.

We set the number of basis fields in the LMC model in eq. (5) to  $B = 10$  in all analyses. The number of fields has to be large enough to allow the LMC model to express complex spatial structures over dialect fields. The  $B$  values selected are “large enough”, in the sense that not all the basis fields are needed: the posterior distribution for some basis fields concentrates on zero; the model has captured enough geographical structure with the remaining fields to model the data and any increase in  $B$  would just add redundant basis fields. In fig. 15 we show the  $B = 10$  basis fields for the full dataset and observe that some of the fields are practically flat over the entire region.

The number of inducing points is  $U = 121$  in all analyses. These correspond to the vertices of a homogeneous rectangular grid dividing the region vertically and horizontally into  $10^2$  sections of roughly  $20 \text{ km}^2$ . This reflects a prior belief that  $20 \text{ km}$  is at or below the length scale over which dialectic variation occurs. With these inducing points we could reconstruct variation on shorter scales if it were there, though we would not accurately quantify uncertainty in such structures due to the nature of the approximations we make. The variational setup would in principle allow us to learn the inducing locations as one more parameter in the model. However, this would be computationally demanding as it requires re-computation of covariance matrices at each iteration.

Parameter	Dimension	Full dataset	Small dataset
$\mu$	$I$	71	8
$\zeta$	$I$	71	8
$a$	$\sum f_i$	741	72
$W$	$B \sum f_i$	7,410	720
$\Gamma(X_{\mathcal{U}})$	$BU$	1,210	1,210
Subtotal (global params)		9503	2018
$X_{\bar{A}}$	$2M$	494	20
Subtotal (with floating locations)		9997	2038
$\Gamma(X_A)$	$BN$	1,200	1,200
$\Gamma(X_{\bar{A}})$	$BM$	2,470	100
Total		13,667	3,338

TABLE 1

Number of parameters in the model. The parameters  $\Gamma(X_A)$  and  $\Gamma(X_{\bar{A}})$  are integrated out of the final posteriors in eq. (16) and eq. (18) using Monte Carlo and the approximation in eq. (12) (these are not output by the Normalizing Flow).

6.2. *Inference via MCMC.* We use Markov chain Monte Carlo (MCMC) methods to perform inference for the LALME model using the small dataset.

Our implementation follows the two-stage MCMC procedure to target the Semi-Modular Posterior (Carmona and Nicholls, 2020) given in section 3.2.3. The two stage approach is needed to deal with the intractable  $\psi$ -dependent normalising constant in  $p(\theta|\psi, Y) = p(Y_{\bar{A}}|\mu, \zeta, a, W, \Gamma(X_{\mathcal{U}}))$ . In order to compare SMPs across different values of the influence parameter  $\eta$ , we repeat this over a grid of values of  $\eta \in [0, 1]$ .

In both stages, we use a standard No U-Turn Sampler (NUTS) (Hoffman and Gelman, 2014) implemented in Blackjax (Lao and Louf, 2020; Lao et al., 2020). This software is convenient for the implementation of the nested MCMC algorithm, as it

allows easily to parallelize the sub-chains in the second stage of sampling thanks to the vectorization capabilities of Jax (Bradbury et al., 2018). Moreover, we can make a reasonable comparison between the cost of inference using MCMC and variational methods by using a shared implementation of the joint log-probability function.

We provide software in our supplementary material.

*6.3. Inference via Variational Methods.* We obtain an approximation to the Semi-Modular Posterior in eq. (16) at each  $\eta \in [0, 1]$ , using the variational methods given in Carmona and Nicholls (2022). In this setup we learn a Variational Meta-Posterior (VMP) which parameterises an approximation to the entire family of SMI posteriors indexed by the influence parameter  $\eta$ . This is similar in spirit to Giordano, Broderick and Jordan (2018); Giordano et al. (2022) who consider perturbations of prior hyper-parameters in variational Bayes posteriors. In contrast we learn the entire family of Variational Meta-Posteriors and vary the influence parameter  $\eta$  indexing the inference scheme. We use a VMP-flow (Carmona and Nicholls, 2022) constructed by composing several 8 conditional coupling layers of Neural Spline Flows (NSFs) (Durkan et al., 2019; Dinh, Sohl-Dickstein and Bengio, 2016) followed by a layer to map the flow into the domain of the model parameters.

In order to construct a variational family for approximation of the SMP in eq. (17), take  $\psi = (\mu, \zeta, a, W, \Gamma(X_{\mathcal{U}}))$  as above, and write the joint variational posterior as

$$(21) \quad q_{\lambda_{1:3}, \eta}(\psi, X_{\bar{A}}, \tilde{X}_{\bar{A}}) = q_{\lambda_1, \eta}(\psi) q_{\lambda_2, \eta}(X_{\bar{A}} | \psi) q_{\lambda_3, \eta}(\tilde{X}_{\bar{A}} | \psi)$$

where  $\lambda_{1:3} = \{\lambda_1, \lambda_2, \lambda_3\}$  are variational parameters which do not depend on  $\eta$  and we use NSFs for each factor. The variational family in eq. (21) depends on  $\eta$  using the parameterisation given in Carmona and Nicholls (2022) which adds  $\eta$  to the conditioner in our coupling-layer conditioner. The trained family of variational densities  $q_{\lambda_{1:3}, \eta}$ ,  $\eta \in [0, 1]$  is called the Variational Meta-Posterior (VMP).

The optimal  $\lambda$ -parameters  $\hat{\lambda}_1, \hat{\lambda}_2$  and  $\hat{\lambda}_3$  maximise a variant of the Evidence Lower Bound (ELBO) as explained in Carmona and Nicholls (2022). A similar revised target utility is given in Yu, Nott and Smith (2021). This modification of the usual variational utility is needed in order to stop the variational approximation introducing uncontrolled information flow between modules. The utilities connecting the Semi-Modular Posterior in eq. (17) to the variational family eq. (21) are

$$\text{ELBO}_{\text{pow}, \eta}(\lambda_1, \lambda_3) = \mathbb{E}_{(\psi, \tilde{X}_{\bar{A}}) \sim q_{\lambda_1, \lambda_3}} [\log p_{\text{pow}, \eta}(\psi, \tilde{X}_{\bar{A}}, Y_A, Y_{\bar{A}}) - \log q_{\lambda_1, \lambda_3}(\psi, \tilde{X}_{\bar{A}})]$$

$$\text{ELBO}_{\text{bayes}}(\lambda_1, \lambda_2) = \mathbb{E}_{(\psi, X_{\bar{A}}) \sim q_{\lambda_1, \lambda_2}} [\log p(\psi, X_{\bar{A}}, Y_{\bar{A}}) - \log q_{\lambda_1, \lambda_2}(\psi, X_{\bar{A}})]$$

and the simplest two-stage variational scheme at a fixed  $\eta$  value would take

$$\hat{\lambda}_1^{(\eta)}, \hat{\lambda}_3^{(\eta)} = \arg \max_{\lambda_1, \lambda_3} \text{ELBO}_{\text{pow}, \eta}(\lambda_1, \lambda_3),$$

$$\hat{\lambda}_2^{(\eta)} = \arg \max_{\lambda_2} \text{ELBO}_{\text{bayes}}(\hat{\lambda}_1^{(\eta)}, \lambda_2).$$

These  $\hat{\lambda}_{1:3}^{(\eta)}$  depend on  $\eta$  so this is not yet the VMP. As explained in Carmona and Nicholls (2022), the two stage scheme can be implemented in a single end-to-end scheme using the stop-gradient operator  $\nabla\!\!\!/(\psi)$ . This ‘‘protects’’ its argument from any derivative in any term in which it appears. The ELBO for the second stage becomes

$$\text{ELBO}_{\text{bayes}, \nabla\!\!\!/(\psi)}(\lambda_1, \lambda_2) = \mathbb{E}_{(\psi, X_{\bar{A}}) \sim q_{\lambda_1, \lambda_2}} [\log p(\nabla\!\!\!/(\psi), X_{\bar{A}}, Y_{\bar{A}}) - \log q_{\lambda_1, \lambda_2}(\nabla\!\!\!/(\psi), X_{\bar{A}})]$$

and the overall utility is

$$(22) \quad \mathcal{L}_{(\text{smi},\eta)}(\lambda_{1:3}) = \text{ELBO}_{\text{pow},\eta}(\lambda_1, \lambda_3) + \text{ELBO}_{\text{bayes},\mathcal{V}(\psi)}(\lambda_1, \lambda_2).$$

In a VMP we learn the variational approximation at each  $\eta$  simultaneously. Following Carmona and Nicholls (2022) we take an auxiliary distribution  $\rho(\eta)$  over  $[0, 1]$  and define

$$(23) \quad \mathcal{L}_{(\text{msmi-flow})}(\lambda_{1:3}) = E_{\eta \sim \rho(\cdot)}(\mathcal{L}_{(\text{smi},\eta)}(\lambda_{1:3})).$$

The optimal variational parameters are then

$$(24) \quad \hat{\lambda}_{1:3} = \arg \max_{\lambda_{1:3}} \mathcal{L}_{(\text{msmi-flow})}(\lambda_{1:3}).$$

These  $\hat{\lambda}_{1:3}$ -values do not depend on  $\eta$  and define  $q_{\hat{\lambda}_{1:3},\eta}$ , the VMP. The optimisations are carried out using the reparameterisation trick and SGD.

We take  $\rho(\cdot)$  to be  $\text{Beta}(1/2, 1/2)$ , reflecting our experience that accurate estimation of the VMP near Bayes and Cut ( $\eta \simeq 0, 1$ ) is important, because the utility  $V(\eta)$  is often rapidly varying in these regions. We will estimate  $\mathcal{L}_{(\text{msmi-flow})}$  using samples  $\eta \sim \rho(\cdot)$ , so taking a continuous density with support on all  $[0, 1]$  but more samples at the extremes is helpful for convergence of SGD over  $\lambda_{1:3}$ . However, NSFs are relatively expressive, and if there exists  $\hat{\lambda}_{1:3}$  maximising  $\mathcal{L}_{(\text{smi},\eta)}(\lambda_{1:3})$  at every  $\eta$  then  $\hat{\lambda}_{1:3}$  also maximises  $\mathcal{L}_{(\text{msmi-flow})}(\lambda_{1:3})$  for *any* distribution  $\rho$  over  $[0, 1]$ , so while  $\rho$  defines the absolute utility of  $\lambda_{1:3}$  it has less impact on the final fitted VMP.

In order to find the value of  $\eta$  maximising the utility  $V(\eta)$  in eq. (20), we target the validation posterior in eq. (18). The variational family targeting the validation-SMP in eq. (18) has the form

$$q_{\lambda_{1:3},\eta}^{(\text{val})}(\psi, X_{\bar{A}\cup\mathcal{K}}, \tilde{X}_{\bar{A}\cup\mathcal{K}}) = q_{\lambda_1,\eta}(\psi) q_{\lambda_2,\eta}(X_{\bar{A}\cup\mathcal{K}} | \psi) q_{\lambda_3,\eta}(\tilde{X}_{\bar{A}\cup\mathcal{K}} | \psi).$$

Having estimated  $q_{\hat{\lambda}_{1:3},\eta}^{(\text{val})}$  as a function of  $\eta$  using the same methods as for  $q_{\hat{\lambda}_{1:3},\eta}$ , we choose  $\eta$  to minimise the loss in eq. (20). This loss function is approximated by taking the variational-posterior Mean Squared Error of the reconstructed anchor locations,

$$(25) \quad V^{(\text{val})}(\eta) = K^{-1} \sum_{p \in \mathcal{K}} \mathbb{E}_{q_{\hat{\lambda}_{1:3},\eta}^{(\text{val})}} \left[ \|x_p - X_p^*\|^2 \right]$$

and then  $\eta^*$  is estimated by simply evaluating this at a selection of  $\eta$ -values.

**6.4. Hyper-Parameters Optimisation (HPO).** We used Hyper-Parameter Optimisation to select a few parameters used for training the model. In particular, we selected four quantities: the decay factor and peak value for the AdaBelief learning rate schedule (Zhuang et al., 2020), as well as the amplitude and length scale for training the Exponential Quadratic kernel for the GP prior of basis fields. The target metric to minimise was the Mean Squared Error defined in eq. (25) using the validation data setting described above. Search was performed via Bayesian Optimisation (BP) (Snoek, Larochelle and Adams, 2012) implemented in the Syne Tune library (Salinas et al., 2022), and executed in 40 distributed training jobs using Amazon SageMaker (Perrone et al., 2020). A pleasing observation during the optimisation process was that the metric values stayed in a stable narrow range after a few ( $\approx 10$ ) iterations.

**7. Data Analyses.** In this section we present our experimental results for the LALME model in section 4.

Our discussion will proceed in an incremental complexity. We start with a conventional Bayesian analysis which estimates the Bayes posterior on floating profiles using the small dataset via MCMC. This is useful for comparison with our later analysis on the full dataset. We then give the VMP and MCMC approximations to the SMI-posterior in eq. (16) for the predicted locations of floating profiles using the small dataset. We trust the MCMC to give a reasonable summary of this SMI-posterior at any fixed  $\eta$  so this gives a check on the VMP: is our NSF sufficiently expressive, and our ELBO-maximisation via SGD sufficiently accurate, to reproduce the ground truth distributions given by MCMC on a dataset small enough to allow MCMC simulation in reasonable time? We illustrate the difficulties with MCMC using the medium dataset.

Having established our methods on the small dataset we then apply them to the full dataset where MCMC is not feasible. We select the influence parameter  $\eta$  using the validation dataset. The same analysis is used to measure the accuracy of our location estimates for the held-out anchors. We then present the results of variational inference on the full dataset with the Semi-Modular Posterior at the optimal  $\eta$ -value.

*7.1. Conventional Bayesian Posterior on the Small dataset.* We start off with a small baseline to assess our model in a manageable setting. The small dataset is obtained by taking 8 items, all 120 anchors and 10 floating profiles from the full dataset. With fewer items we require fewer dialect basis fields, and this gives a helpful reduction in parameter dimension. With a small number of floating profiles, the fields are mainly informed by the anchor locations, reducing any damage due to feedback between imputed locations for floating profiles and latent fields.

In this setting, MCMC on the conventional Bayesian posterior in eq. (12) (conditioned on  $Y_{\mathcal{P}}$ ) is satisfactory overall. We observe good mixing for the global parameters  $\mu$  and  $\zeta$  in fig. 6, comparing samples for four chains of the NUTS MCMC sampler. The zeroing probabilities  $\zeta_i$ ,  $i \in \mathcal{I}$  are not small, ranging from around 0.3 to 0.7. The mean useage frequencies  $\mu$  vary from around 5 to 15. Marginal posterior location-distributions for a subset of 10 representative floating profiles are displayed (in blue) in fig. 7, and their corresponding traces for northing and easting coordinates in fig. 8. We select 10 floating profiles which “cover” the window  $\mathcal{X}$  (using the Atlas location estimates to guide our choice) as we expect different behaviour in different sectors due to the uneven distribution of anchors (see fig. 1).

We observe some issues with convergence and mixing of some chains for the floating locations even in this small-data setting. For example, chains for coordinates of profiles 699 and 755 (last two rows from top in fig. 8 and bottom right corner of the grid in fig. 7) move very slowly between different modes. The problem gets worse if we increase the number of floating profiles or the number of items. We ran an experiment using the medium dataset, including all floating profiles but still only 8 items. We display MCMC traces in fig. 16. These mixing problems with the floating locations are related to the issues reported by Haines (2016), which may be caused by mis-specified feedback between floating profile locations  $X_{\bar{A}}$  and linguistic fields  $\Phi$ . These mixing problems are not observed when the MCMC targets the Cut distribution, with corresponding traces display in the Appendix fig. 8. Although the MCMC might of course be improved, the VMP offers other advantages besides stable estimation. Separate runs at different  $\eta$  values are not required as the VMP parameterises a smooth sequence of SMI-posteriors over  $\eta \in [0, 1]$  in a single end-to-end training scheme.

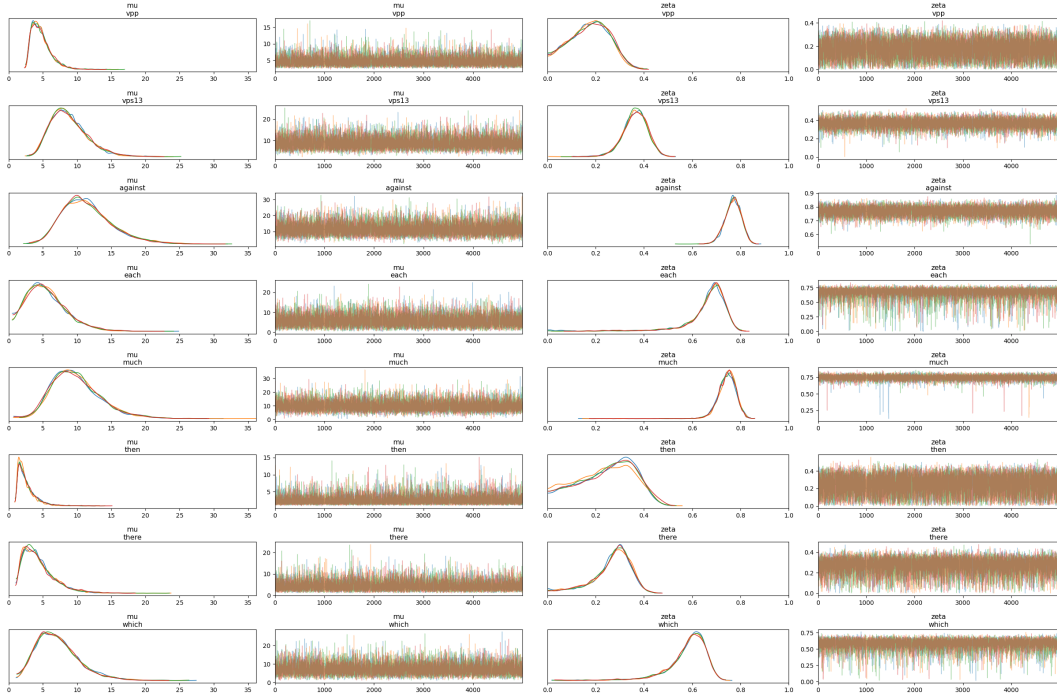


Figure 6: Distributions and trace plots for  $\mu_i$  (left) and  $\zeta_i$  (right),  $i = 1, \dots, I$ . We compare four MCMC chains targeting the conventional Bayesian posterior (eq. (12) or equivalently  $\eta = 1$  in eq. (16)) on the small dataset.

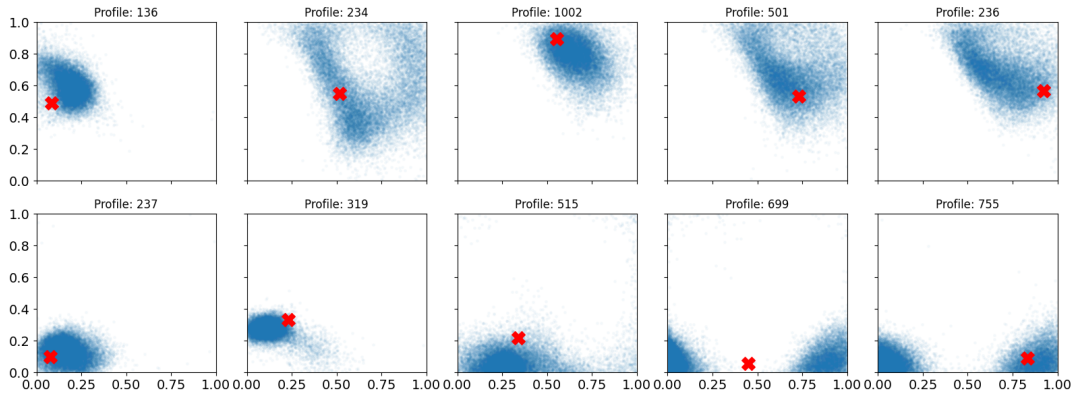


Figure 7: Posterior samples (in blue) for the 2D locations of a subset of floating profiles. The samples correspond to the Bayesian posterior on the small dataset. The red cross indicates the Atlas location estimated using the fit-technique. Samples are output from MCMC targeting eq. (12) or equivalently  $\eta = 1$  in eq. (16).

7.2. *Variational SMI on the Small dataset.* We now expand the analysis to consider the Variational Meta-Posterior on the small dataset. The purpose of this section is show that the Variational Meta-Posterior we fit shows reasonable agreement to the MCMC ground truth for the SMI-posterior at each  $\eta$ -value.

We observe good agreement for global model parameters. Comparisons of the SMP for  $\zeta$  and  $\mu$  determined by the VMP at  $\eta$ -values 0, 0.25, 0.75 and 1 are shown in fig. 9

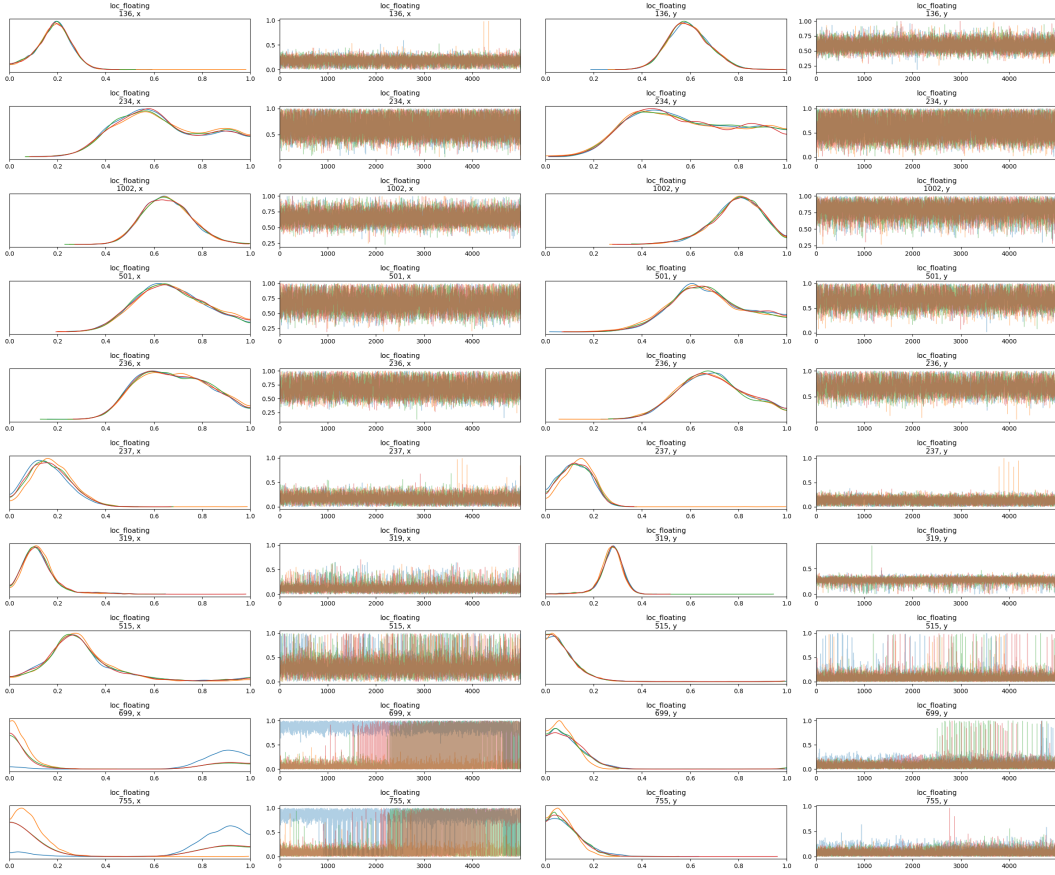


Figure 8: Distributions and trace plots for a subset of floating locations. We compare four MCMC chains for the conventional Bayesian posterior ( $\eta = 1$ ) on the small dataset.

and fig. 10 respectively. The VMP concentrates on similar ranges for the two methods, across items and along degrees of influence  $\eta$ . The variational SMP is narrower, as one would expect from variational approximations. Our approximation based on Neural Spline Flow alleviates part of the underestimation of variance that one would observe with less expressive families such as a Mean Field parametrisation. The distributions of these global parameters are insensitive to  $\eta$ , showing that they get relatively little information from the floating profiles.

The approximation to the posterior locations of floating profiles is also good overall. In fig. 11 we overlay Highest Posterior Density (HPD) credible regions (with levels 0.05, 0.5, 0.95) of the variational posterior for the locations of ten representative floating profiles at  $\eta$ -values 1, 0.75, 0.25 and 0. The top grid of plots in fig. 11(a) corresponds to the Bayes posterior ( $\eta = 1$ ) and are identical to those in fig. 7. The bottom grid of plots fig. 11(d) corresponds to the Cut Posterior ( $\eta = 0$ ), which completely eliminates feedback from the floating profiles. Other values of  $\eta$  interpolate between the Cut and Bayes posterior, allowing partial feedback from the floating profiles. The main posterior modes are recovered, with no evidence for under-dispersion, and we find agreement even in complex multi-modal structures (for example profile 755, far right in the bottom row of grids a-d). However, there are also regions of disagreement, (for example profile 699, second from right in the bottom row of grids a-d, where a mode is missed) including

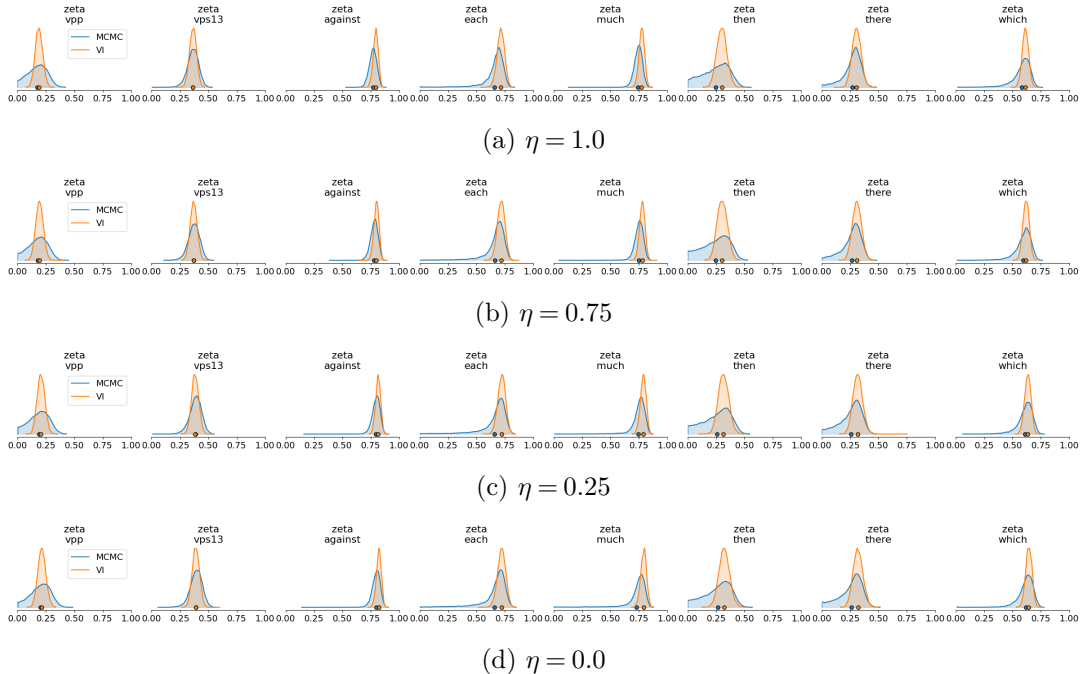


Figure 9: Comparison of the SMP distributions for  $\zeta$  on the small dataset across different values of  $\eta$ . We compare the MCMC samples (blue) with the Variational posterior approximation (orange).

regions frequently visited by the MCMC chain where the variational posterior do not assign high probability.

*7.2.1. Variational Inference on the full dataset.* We now consider the analysis of the full data. This is done in two stages. First we fit the validation dataset, visualise the results (in fig. 12) for prediction of held-out anchors, and then select the optimal influence parameter  $\eta^*$  to minimise the variational-posterior MSE (in fig. 13). We then refit the VMP to the full dataset using the utility in eq. (23)) and report selected posterior distributions for the locations of floats, predicted now using all the anchors and the optimal level of influence (in fig. 14).

The comparison of our variational approximations in section 7.2 with MCMC “ground truth” gave good results in general for the small dataset. The SMP distributions for global parameters and many profile locations were well represented, and the distributions of most profiles were accurately captured. It is important to bear in mind that in the setting with a large number of floating profiles, multiple disconnected modes may be present in the posterior of imputed locations, which complicates inference for both MCMC and VI. However, the VMP location distributions are in pleasing agreement with the Atlas float-locations assigned by the fit-technique (association of red crosses and contours in fig. 11) and this suggests the variational approximation may give useful location predictions. We cant use Atlas locations for floats for inference purposes. Fortunately, as discussed in section 5.1, we can use held-out anchor profiles to quantify the accuracy of the SMP location distributions estimated using the VMP.

In fig. 12 we plot (in the same format as fig. 11) the marginal distributions  $q_{\lambda_{1:3},\eta}^{(val)}(x_p)$ ,  $p \in \mathcal{K}$  (see definition the end of section 6.3) of fifteen of the  $K = 20$  held-out anchors for  $\eta$ -values 1, 0.75, 0.25 and 0. These  $\eta$ -values are chosen for illustration

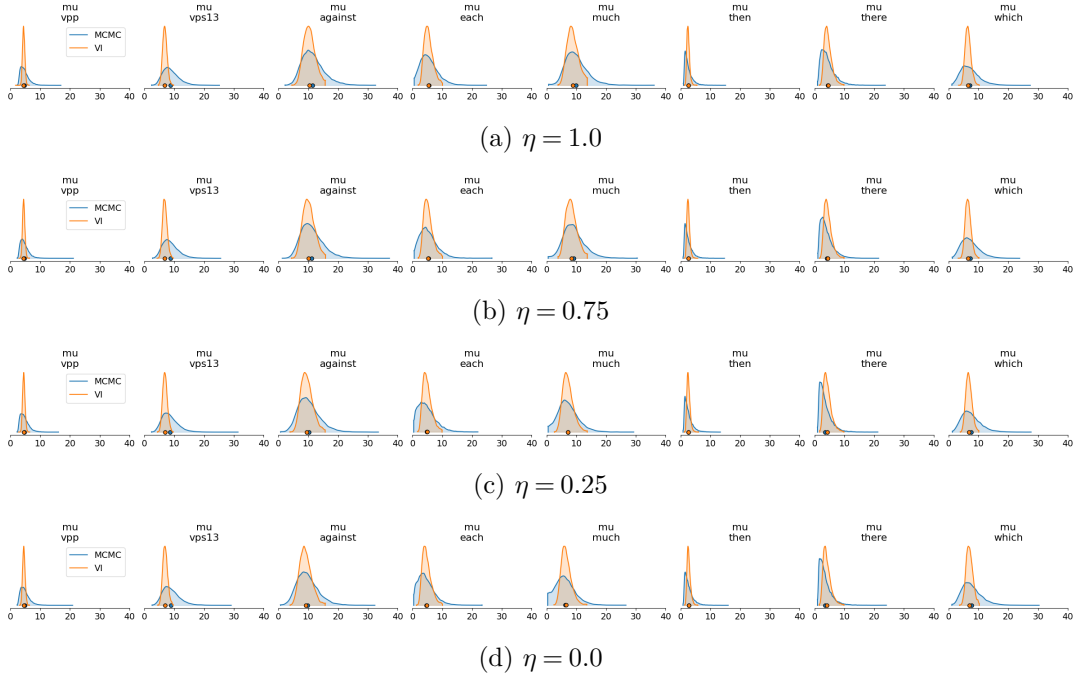


Figure 10: Comparison of the SMP distributions for  $\mu$  on the small dataset across different values of  $\eta$ . We compare the MCMC samples (blue) with the Variational posterior approximation (orange).

as the estimated loss  $\hat{V}^{(val)}(\eta)$  has a minimum at around  $\eta = 0.7$ . We draw attention to three features of this figure. First, the locations of the held-out anchors are clearly well-predicted by the marginal posteriors at each  $\eta$ . Second, the distributions tend to become more diffuse as we move down through the grids from (a) to (d) becoming really quite diffuse in the cut model in (d). This shows that the information in the floating profiles is informing the fields  $\Phi$  at larger  $\eta$  values where some modulated feedback is allowed. Third, the distributions in fig. 12 are more uni-modal in appearance than those those in fig. 11. We believe this shows the usual concentration of the posterior with increasing data (here both  $I$ , the number of items and  $M$  the number of floating profiles have increased). This means it is likely that the variational approximations are more accurate than those in section 7.2 as the target is more easily matched.

We now present results for the choice of  $\eta$ . The loss  $V^{(val)}$  is estimated by sampling  $q_{\hat{\lambda}_{1:3},\eta}^{(val)}(x_p)$ ,  $p \in \mathcal{K}$  and averaging. The  $\eta$ -dependence of  $\hat{V}^{(val)}(\eta)$  is plotted in fig. 13 at left. It has a minimum at around  $\eta \approx 0.7$ . Given the generally uni-modal shape of the marginal posterior location distributions in fig. 12, the posterior mean is a reasonable estimator. At right in fig. 13 we plot

$$(26) \quad K^{-1} \sum_{p \in \mathcal{K}} \left\| \bar{x}_p - X_p^* \right\|$$

with  $\bar{x}_p = \hat{\mathbb{E}}_{q_{\hat{\lambda}_{1:3},\eta}^{(val)}}[x_p]$ . This measures the distance between point prediction and truth, as it removes the effect of posterior dispersion present in  $V^{(val)}$  but remains sensitive to all the biasing effects of model mis-specification. The resulting estimated average misplacement distance for location prediction of the held out anchors is around 28

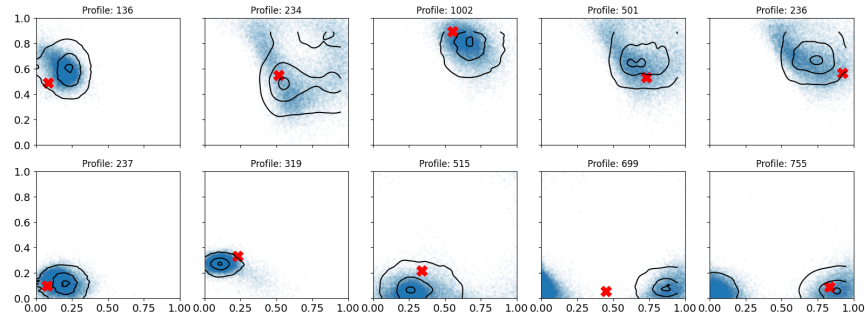
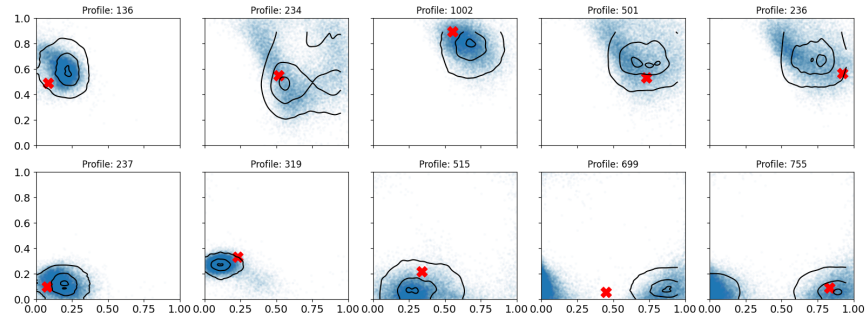
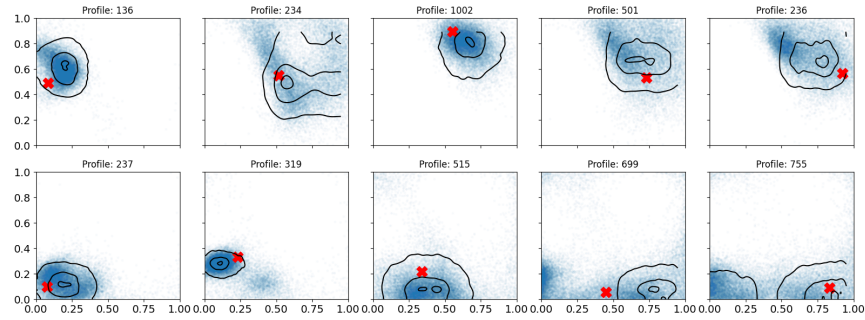
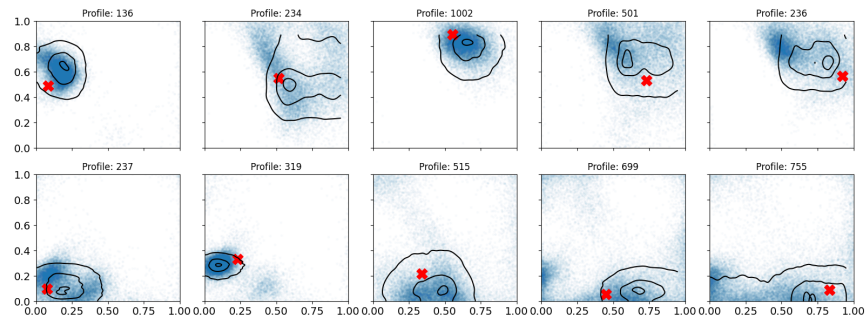
(a)  $\eta = 1.0$ (b)  $\eta = 0.75$ (c)  $\eta = 0.25$ (d)  $\eta = 0.0$ 

Figure 11: Posterior distributions of ten floating locations obtained using SMI with varying values of  $\eta$ . Small Dataset. Red cross denotes the floating-profile location assigned by the fit-technique. We compare the MCMC samples (blue scatter plot) with the Variational Meta-Posterior approximation (level sets at levels 0.05, 0.5, 0.95).

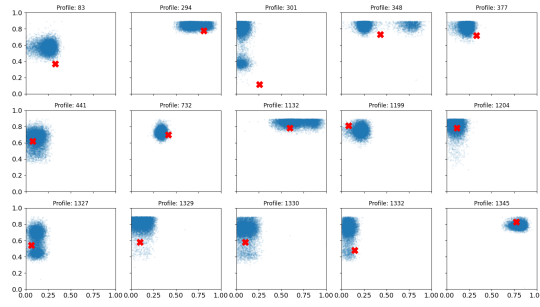
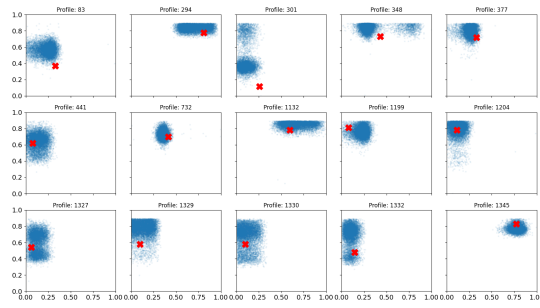
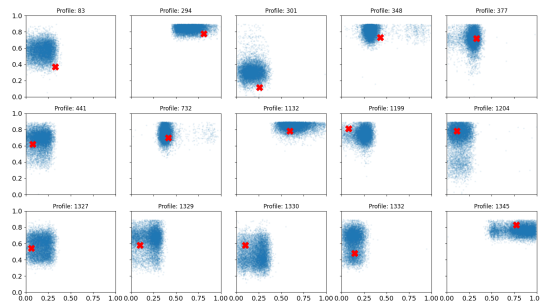
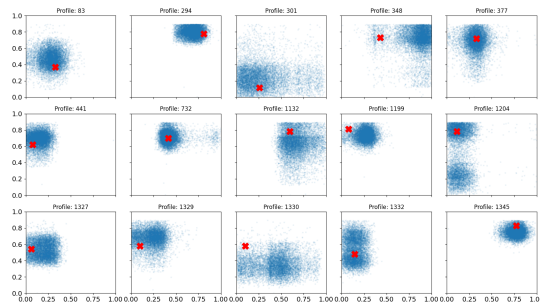
(a)  $\eta = 1.0$ (b)  $\eta = 0.75$ (c)  $\eta = 0.25$ (d)  $\eta = 0.0$ 

Figure 12: Posterior distributions of imputed locations for fifteen (random) held-out anchor profiles obtained using the Variational Meta-Posterior on the entire LALME dataset. Darker regions denote higher posterior probabilities, and red crosses mark true locations of profiles.

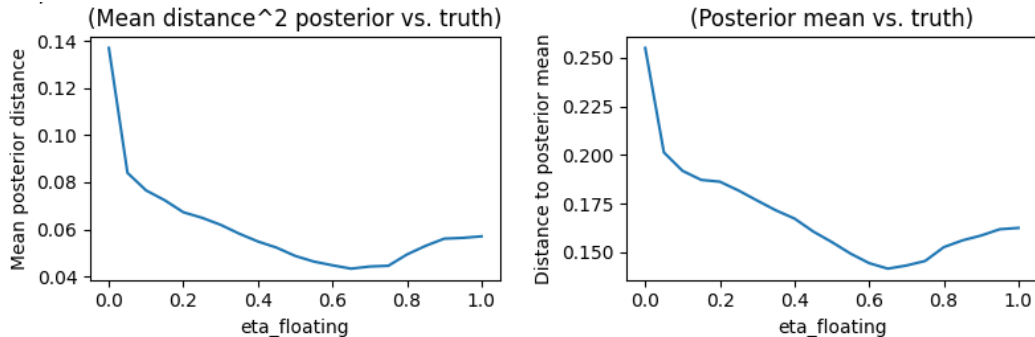


Figure 13: Error in location reconstruction for held-out profiles as a function of the influence parameter. Left: Variational-posterior MSE to true location, in eq. (25). Right: Euclidean distance between the true location and the posterior location mean, in eq. (26). In both cases, we average over twenty random held-out profiles, including those shown in fig. 12. The best Semi-Modular Posterior is obtained with  $\eta \approx 0.75$  producing an average held-out error of around  $200 \times 0.15 = 30$  km on point estimates in our  $200 \times 180$  km<sup>2</sup>.

kilometres and we take this as our estimate of the scale of the error for our prediction of locations for floating profiles in fig. 14 below.

In the last stage of this analysis, we refit the VMP to the posterior in eq. (16) for the full dataset and plot marginal posterior distributions for the locations of selected profiles along with the atlas locations in fig. 14. This is the main “output” result of this paper. The optimal influence  $\eta^*$  lies somewhere between grids (b) and (c). The distributions (in blue) are somewhat more concentrated than those for the held-out anchors in fig. 12. This may reflect differences in the text-type. Anchors are generally short legal documents with locations indicated in the text and relatively few items. Unlocated texts corresponding to floating profiles are often book-length texts, with a much wider range of items. Also, the disagreement between posterior distributions for float locations and Atlas fit-technique locations is somewhat larger than that seen for held out anchors. However, the fit-technique is itself subject to uncertainty so this is to be expected.

The VMP-means for the basis GP fields  $\Gamma$  offer some insight on the real underlying structure of the form-probability fields  $\Phi$ . These are plotted in fig. 15 at the same selection of  $\eta$ -values. The scales given by the shading-bar to the right of each graph are important here. For example, in the bottom row of plots, corresponding to the cut at  $\eta = 0$ , the scales for graphs 1,3,4,5,9 (reading from left) show that the fields show small or negligible variation across the region  $\mathcal{X}$ . These basis fields could be dropped from the analysis with relatively little loss in the quality of the fit. As we move down a column we see the basis field evolves, though retains its basic form. The basis fields have a label switching symmetry in the posterior, but VMP is helpfully breaking that symmetry and identifying fields across  $\eta$ -values: the same set of  $\hat{\lambda}_{1,3}$ -values are used in each posterior. Fields six and ten capture variations which are aligned roughly north-south and east-west respectively. We conjecture that this reflects the imprint of the population history of speakers in this region on the spatial patterning of dialect.

## 8. Conclusions.

8.1. *Main results.* We have shown how to simultaneously estimate spatial fields and measurement locations using a set of anchored measurements. We selected an inference

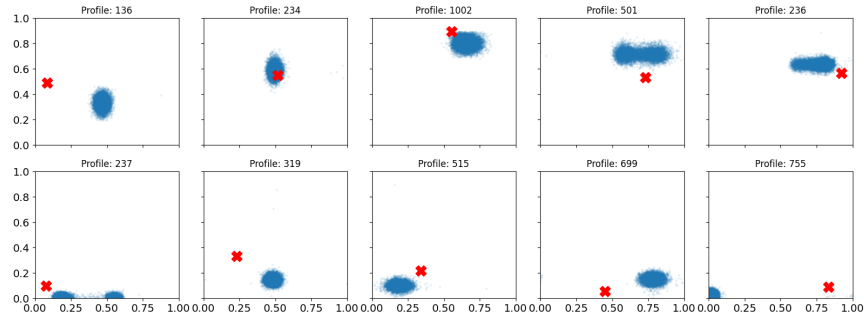
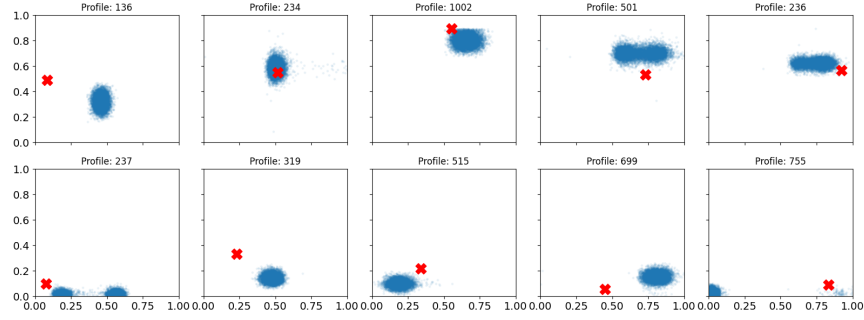
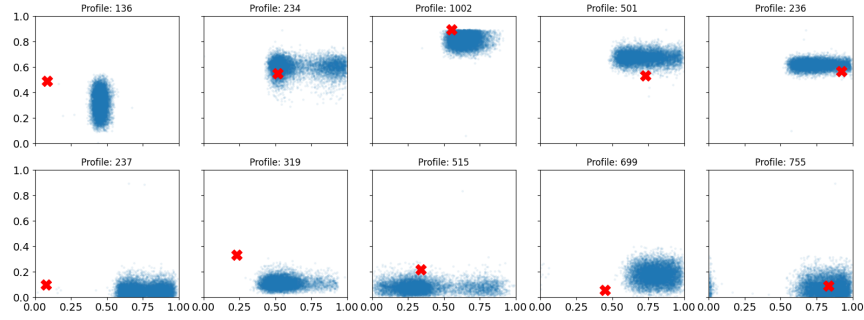
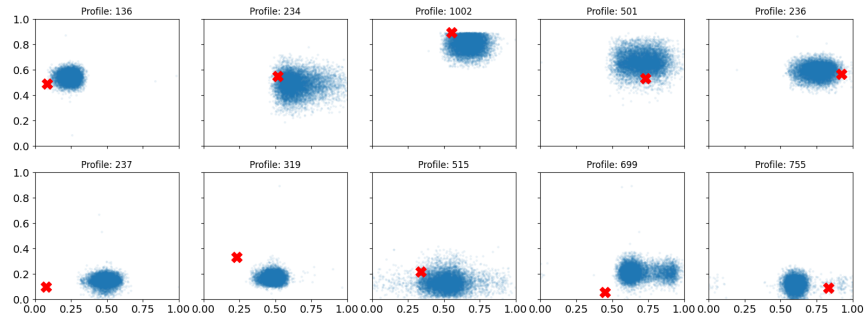
(a)  $\eta = 1.0$ (b)  $\eta = 0.75$ (c)  $\eta = 0.25$ (d)  $\eta = 0.0$ 

Figure 14: Posterior distributions of locations of ten randomly chosen floating LPs, obtained using Variational Meta-Posterior with varying values of  $\eta$ . Darker regions denote higher probabilities on each plot, and red crosses mark location assigned by the fit-technique.

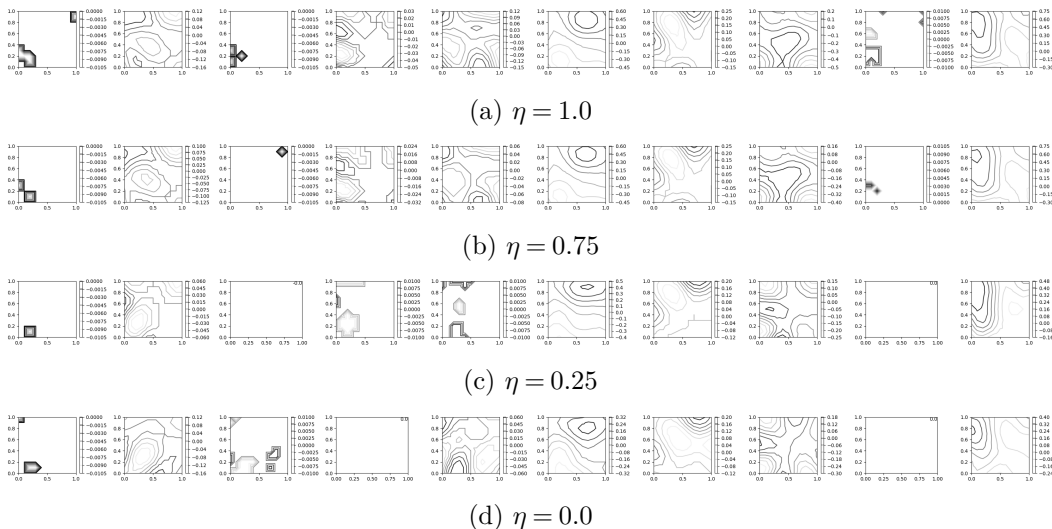


Figure 15: Visualization of the posterior basis GP fields  $\Gamma$ , represented by the level plots of the Semi-Modular Posterior mean. Darker lines denote higher levels within each plot. We set the number of basis fields equal to 10, but observe from the scale bars that the posterior concentrates on a smaller number of *effective* basis fields, leaving a few flat fields (eg. first field in every row).

framework (from Cut models and SMPs and the Bayesian posterior) which makes some allowance for mis-specification. This methodology is needed due to the high-dimension of the missing data (the fields) and the difficulty of forming an accurate generative model for the data. The selected value of the influence parameter is less than one. Referring to fig. 12, this makes sense: the posterior distributions clearly cover the true held-out anchor locations more reliably at  $\eta$  values smaller than one. This confirms that some down-weighting of the information from floating profiles is desirable.

Was it worth it? Does information from the floating profiles actually help our statistical analysis? One could simply infer the posterior distribution of the spatial fields from the anchors and use this to predict float locations. This would be cut-model inference and corresponds to the bottom grid in fig. 12 with  $\eta = 0$ . Whilst these marginal posterior distributions do cover the true values well, they are clearly much more diffuse than the distributions in the grid at larger  $\eta$ , as they throw out all information from the floats. This shows that allowing some feedback is useful.

One nice feature of the inference framework here is the possibility of using the location error itself as a loss for selection of the influence parameter  $\eta$ . Previous work used the elpd as a guide. This reflects that fact that the location parameters  $x_p$ ,  $p \in \bar{A}$  are “physical” quantities, with a clear meaning independent of the model, mis-specified or otherwise. In fact a loss of this sort will be available in many problems that have the form of supervised classification: if  $x_p$  is the “class label” for observation  $p$  and  $y_p$  is a feature vector then  $x_p$  are known in the training data  $p \in A$  and unknown in the unlabelled data  $p \in \bar{A}$  intended for classification. In our case the class labels are continuous, but the physical meaning for the labels, and the possibility for constructing a loss minimising the predicted classification error, remains.

Our final results in fig. 14 show our predictions for the locations of floating profiles. These profiles were selected to cover the region, and are representative of typical

performance. There is good agreement between our predicted locations and those established using the fit technique. We provide a formal quantification of uncertainty missing in that non-statistical method. The application we have given was selected to demonstrate the effectiveness of our method and agreement with the Atlas. Our methods could be used to predict the location of new profiles. From the perspective of users this would be the main application of interest. In principle this should be done by adding the new profile to the set of floats and repeating the simulation in section 7.2.1. However, a single profile is unlikely to change the distribution to any great degree, so treating the existing analysis as the first stage of a cut model for Bayesian multiple imputation of  $\psi$ , and considering the posterior distribution of the new profile location conditioned on its  $y_p$ -values and the imputed (random) fields, should lead to efficiency gains with little loss of accuracy.

What really was the mis-specification? The generative model given in this paper is a significant improvement on that in Haines (2016), we believe because of the reduction in field dimension due to working with basis-fields, and the natural way this introduces correlation between fields. However, we ignored correlation between the forms of an item selected by a scribe. They are unlikely to use multinomial sampling of forms. Also, where a scribe is copying a text in an alien dialect, they may sometimes copy the spellings of that text (cf. Benskin and Laing, 1981); though the authors of LALME sought as a matter of principle to exclude such mixed language from the maps, they may not have recognised every instance. This may bring forms from far afield into the profile. Finally, locations are not missing completely at random from the LPs: anchor texts tend to be derived from legal documents whereas the floating LPs represent a great variety of texts. There are no doubt other processes which we do not understand. The use of an inference framework that accommodates these errors, rather than further model-elaboration, allowed us to make progress without ultimately resolving these issues.

8.2. *Future work.* Our Semi-Modular analysis reduces the influence of all floating profiles homogeneously by using a single common influence parameter. Nevertheless, there are other possible ways to *modularize* our probabilistic model for the LALME data. Two extensions may be of interest for future exploration. First, we could reduce the influence of individual profiles differently, replacing  $\eta \rightarrow \eta_p$ ,  $p \in \bar{A}$ . This would be equivalent to introducing *multiple cuts* in the model, and in practice could be achieved by imposing different powers  $\eta_p$  on the likelihood of each profile. This would require an elpd-style training loss for  $\eta$  selection. Second, we could reduce the influence of some items. The geographical structure may be more marked for some items, they may be more informative and associated observations more easily modelled. Some words are clearly differentiated by region, while others may be used equally across regions. We may find we can improve our location accuracy by reducing the influence of unstructured or mis-specified items. This case would also entail multiple cuts and would be implemented by introducing a set of influence-parameters  $\eta_i$ ,  $i \in \mathcal{I}$  to be applied as per-factor powers in the likelihood product over items. Carmona and Nicholls (2022) shows how a loss on multiple cuts may be optimised in a VMP setting using SGD.

## APPENDIX A: FURTHER BACKGROUND ON THE DATA

**A.1. LALME.** The Linguistic Atlas of Late Mediaeval English (McIntosh, Samuels and Benskin, 1986; Benskin et al., 2013) is a survey of local variation in the written language for the period c. 1350 to c. 1450. Its results are presented as separate maps for each of 62 selected items. Here an “item” is a word or other linguistic category, such as a grammatical inflexion or an etymological segment, here marked by  $\{\}$ ; the variant realisations of an item are its “forms”, here marked by  $\langle \rangle$ . An item map displays all of the variant forms for that item as recorded at the irregular grid of survey points shown as red and blue dots in fig. 1. Additionally, and for the same survey points, twelve hundred dot maps report the distributions of select variants or sets of variants for another 218 selected items, as well as analyses of such distributions within the item maps.

The survey includes most of England and such few parts of Wales from which English writing is known, and provides token coverage of southern Scotland. Scotland is now treated comprehensively by Williamson (2008). Ideally the period of survey would be much less, to guard against interference from variation over time with variation over space, but the accidents of manuscript production and survival, and the displacement of local usage by what was becoming a national written standard, would leave large areas unrepresented if this time-span were much reduced (McIntosh, 1963; McIntosh, Samuels and Benskin, 1986). Even so, and in spite of the 1044 profiles entered on the maps, coverage for England remains geographically uneven; for parts of the north and the south-west it is very sparse, whereas for East Anglia, the London area, and parts of the West Midlands, there is little room for additional material.

**A.2. Survey points and the fit-technique.** The Leeds Survey of Modern English Dialects (Orton and Dieth, 1962) could choose its three hundred survey points as more or less evenly spaced across the land, but a survey of the mediaeval language has to make the best of what it can find. The Atlas’s ‘informants’ were its sample manuscripts, represented by 1044 linguistic profiles. An additional challenge is that the local origins for the bulk of these informants were at the outset unknown: the Atlas had to be constructed as an ever-tightening taxonomic matrix within which unlocalised informants could be placed. Since regional dialect changes for the most part in an orderly way over space (that is, the regional distributions of dialectal features are for the most part cohesive), it follows that a taxonomic placing within a geographically rooted irregular grid is an approximation to a local origin, and the denser the grid, the more closely will that origin be defined; informants so placed can be incorporated as additional survey points, and contribute in their turn to the placing of others. This procedure - McIntosh’s fit-technique (McIntosh, 1963; Benskin, 1991; McIntosh, Samuels and Benskin, 1986)- defines relative placings within a grid variously anchored by informants for which there is good non-linguistic evidence of local origin. In rare cases, a scribe can be identified and his biography is known, but most anchors are legal or administrative documents whose place of origin is explicitly stated, and which (though it is not a foregone conclusion) can be trusted at least provisionally to represent the local forms of language (Benskin, 2004). In one or two cases, anchors found after the Atlas was published have confirmed placings previously determined by ‘fit’.

The fit-technique is mechanical and cartographic, proceeding from a set of maps each of which displays the geographical distributions of the variant forms for a single item. A local dialect can be regarded as an assemblage of such forms, some few of which may be confined to that assemblage, but most if not all of which are shared with one or another of the neighbouring dialects; a local dialect is thus far an intersection of the distributions

of its constituent forms. The local usage in any of the Atlas inhabited blank spaces is hence assumed to have been a sub-set of the aggregate of the forms in the survey points that delimit that space, with few of its forms (if any) that are not predictable from those delimiters. Conversely, when such a combination is identified, it is assumed, in default of evidence to the contrary, to represent the local usage proper to that space (McIntosh, Samuels and Benskin, 1986). The fit technique treats dialectal distributions in terms of areas and overlaps, and proceeds by the cumulative elimination, map by map, of all the areas which are documented but in which the constituent features of the unlocalised dialect are not recorded. What remains is the area which accommodates all its features as an assemblage; in the first instance it is a taxonomic sector, and by implication the dialect's area of origin. The present paper considers a statistical alternative to this procedure.

**A.3. Linguistic profiles.** The core of the Atlas comprises some 1044 taxonomic inventories, whose contents are the spellings elicited by a fixed-format survey questionnaire; a completed survey questionnaire is a linguistic profile ('LP') for an individual scribe. In all, the forms of 623 distinct items were recorded. The items were unevenly surveyed over space. Details of how the list of recorded items developed are recorded in the Atlas. It should perhaps be emphasised that the survey is not concerned with peculiar local vocabulary. The choice of an item was governed by two considerations: (a) it must be represented by at least two co-variant forms of philological interest, and (b) it must be in common use, with a good chance of appearing in whatever text might be available. Most items are hence commonplace vocabulary, like {THESE}, {SHE}, {WHICH}, {SHALL}, {IF}, {TOGETHER}, and {TWO}. Grammatical inflexions are almost by definition of common occurrence; among those used in Atlas are the suffixes of the {present participle} (so <~ING>, <~YnG>, <~AND>, <~END>, etc.) and the {noun plural} (so <~ES>, <~IS>, <~US>, etc.). The Atlas is in the first instance a survey of written language: much of the variation it records corresponds to variation in the spoken language, but some of it, like that between <~YnG> and <~ING>, demonstrably does not. The idea that any given word in English should have one and only one spelling, even if its pronunciation was a constant, was alien to perhaps the majority of scribes; spelling systems had their own generative logic, which could be developed in different ways. Although some scribes were very consistent, it is not unusual to find in the course of a long text that many words, perhaps even a majority, have several forms in either free or conditioned variation. Since the Atlas was intended as a research tool, all variants elicited by the questionnaire, regardless of their presumed significance for the spoken language, are separately recorded; transcribed from manuscript, they are represented in raw state so far as conversion into ASCII characters allows. The contents of the completed survey questionnaires are correspondingly prolific and diverse.

**A.4. Coarsening.** The number of forms corresponding to a single item can be very large, commonly in the range of 100–200; notorious is {THROUGH}, for which the Atlas records over four hundred variants. After analysing this primary data, Haines (2016) adopted a coarsened version, in which the forms of an item under consideration were classified and treated as subsets. For experiments with multi-dimensional scaling as an alternative to the 'fit'-technique (Benskin, 1988), a segmentation dictionary had been developed in course of making the Atlas. For each item, a template consisting of vowel and consonant segments was devised from which all of its variants could be generated. For example, the template for {THEM} is C1+V1+C2+V2+C3. These can be seen as slots into which particles can be dropped. In {THEM}, C1 can be null (in the

forms ⟨AM⟩ and ⟨EM⟩) or H (so ⟨HAM⟩, ⟨HEM⟩, etc.) or TH (so ⟨THEM⟩, ⟨THAIM⟩, etc.) or the mediaeval ‘thorn’ (so ⟨yEM⟩, ⟨yEIM⟩, etc.) or mediaeval ‘yogh’ (for which ⟨zAM⟩, ⟨zEOM⟩, etc.); V1 can be A, E, EE, EO, I, Y, O, OE, U, UE, EI, EY, AI, AIE, AY; C2 is usually M, but often abbreviated (so ⟨HEm⟩, ⟨THAm⟩, etc.), rarely MM (for example ⟨HEMME⟩) or mM (for example ⟨yAmME⟩), but can be S (seen in ⟨AS⟩, ⟨ES⟩, ⟨HIS⟩, etc.) or N (as ⟨HAN⟩) or NN (in ⟨yENN⟩); V2 is usually null, but may be E (as in ⟨THAIME⟩); C3 is usually null, but may be M (in ⟨HEMEM⟩) or N (in ⟨HYMEN⟩). These do not exhaust the possibilities for the 116 different forms (letters may be written superscript, as for example in ⟨HA<sup>A</sup>M⟩ and ⟨Y<sup>EM</sup>⟩), but are enough to demonstrate the principle. Via such a template, comparison of LPs in respect of them can be confined to a single segment, and the number of variants reduced to easily managed proportions by identifying different particles within a slot. Thus for C1, a binary contrast of H versus TH and its mediaeval equivalent ‘thorn’ includes most by far of the 116 variants and so removing the distinction between H and TH in C1 of {THEM} is a coarsening; the contrast is implicitly phonological, as is that between M (including abbreviated m) and S for C2. Philological judgement, by no means infallible, is called for at every stage, but such restrictions relieve the input data of what is likely to be a great deal of noise.

For present purposes, the area investigated was also confined. We focus on a rectangular area spanning 200km east-west and 180km north-south, as displayed in fig. 1. This contains 120 anchor Linguistic Profiles (LPs) and a further 247 floating LPs that have been assigned locations via the fit-technique.

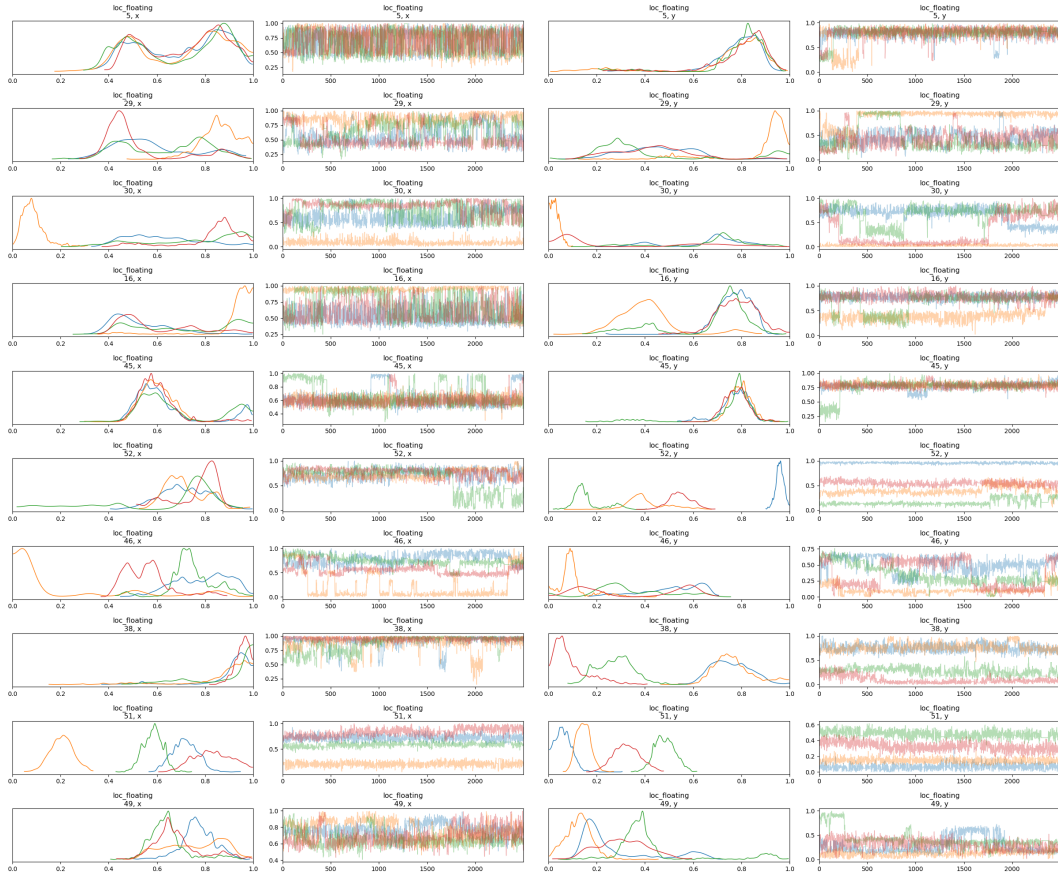


Figure 16: Distributions and trace plots for a subset of floating locations. We compare four MCMC chains for the conventional Bayesian posterior ( $\eta = 1$ ) on the medium dataset including all (247) floating profiles and 8 items.

## REFERENCES

- AGLIETTI, V., BONILLA, E. V., DAMOULAS, T. and CRIPPS, S. (2019). Structured Variational Inference in Continuous Cox Process Models. In *Advances in Neural Information Processing Systems* **32**. Curran Associates, Inc.
- BANERJEE, S., CARLIN, B. P. and GELFAND, A. E. (2014). *Hierarchical Modeling and Analysis for Spatial Data*, 2 ed. Chapman and Hall/CRC, New York.
- BENSKIN, M. (1982). The letter <þ> and <y> in later middle English, and some related matters. *Journal of the Society of Archivists* **7** 13–30. Publisher: Routledge.
- BENSKIN, M. (1988). The numerical classification of languages, and dialect maps for the past. In *Distributions spatiales et temporelles, constellations des manuscrits/Spatial and Temporal Distributions, Manuscript Constellations: Etudes de variation linguistiques offertes à Anthonij Dees à l'occasion de son 60ème anniversaire / Studies in language variation offered to Anthonij Dees on the occasion of his 60th birthday* (P. v. Reenen and K. v. Reenen-Stein, eds.) John Benjamins Publishing Company Pages: 13 Publication Title: Distributions spatiales et temporelles, constellations des manuscrits/Spatial and Temporal Distributions, Manuscript Constellations: Etudes de variation linguistiques offertes à Anthonij Dees à l'occasion de son 60ème anniversaire / Studies in language variation offered to Anthonij Dees on the occasion of his 60th birthday.
- BENSKIN, M. (1991). The "fit" technique explained. In *Regionalism in Late Medieval Manuscripts and Texts: Essays Celebrating the Publication of a Linguistic Atlas of Late Mediaeval English* (F. Riddy, ed.) 9–26. Cambridge : D.S. Brewer.
- BENSKIN, M. (2004). Chancery Standard. In *New Perspectives on English Historical Linguistics Volume II: Lexis and Transmission*, (C. Kay, C. Hough and I. Wotherspoon, eds.). *Current Issues in Linguistic Theory* 21–26. John Benjamins Publishing Company, Amsterdam/Philadelphia.
- BENSKIN, M. and LAING, M. (1981). Translations and Mischsprachen in Middle English Manuscripts. In *So meny people longages and tonges: philological essays in Scots and mediaeval English presented to Angus McIntosh* 55–106. University of Edinburgh ISBN: 0950693820.
- BENSKIN, M., LAING, M., KARAIKOS, V. and WILLIAMSON, K. (2013). An Electronic Version of A Linguistic Atlas of Late Mediaeval. url: <https://www.lel.ed.ac.uk/ihd/elalme/elalme.html>.
- BISSIRI, P. G., HOLMES, C. C. and WALKER, S. G. (2016). A general framework for updating belief distributions. *Journal of the Royal Statistical Society: Series B (Statistical Methodology)* **78** 1103–1130.
- BONILLA, E. V., KRAUTH, K. and DEZFOULI, A. (2019). Generic inference in latent Gaussian process models. *Journal of Machine Learning Research* **20**. arXiv: 1609.00577.
- BRADBURY, J., FROSTIG, R., HAWKINS, P., JOHNSON, M. J., LEARY, C., MACLAURIN, D. and WANDERMAN-MILNE, S. (2018). JAX: composable transformations of Python+NumPy programs.
- CARMONA, C. U. and NICHOLLS, G. K. (2020). Semi-Modular Inference: enhanced learning in multi-modular models by tempering the influence of components. In *Proceedings of the 23rd International Conference on Artificial Intelligence and Statistics, AISTATS 2020* (C. SILVIA and R. CALANDRA, eds.) 4226–4235. PMLR arXiv: 2003.06804.
- CARMONA, C. U. and NICHOLLS, G. K. (2022). Scalable Semi-Modular Inference with Variational Meta-Posteriors. arXiv: 2204.00296.
- CHAKRABORTY, A., NOTT, D. J., DROVANDI, C., FRAZIER, D. T. and SISSON, S. A. (2022). Modularized Bayesian analyses and cutting feedback in likelihood-free inference. arXiv: 2203.09782.
- DIGGLE, P. J., TAWN, J. A. and MOYEED, R. A. (1998). Model-based geostatistics. *Journal of the Royal Statistical Society: Series C (Applied Statistics)* **47** 299–350.
- DIGGLE, P. J., MORAGA, P., ROWLINGSON, B. and TAYLOR, B. M. (2013). Spatial and Spatio-Temporal Log-Gaussian Cox Processes: Extending the Geostatistical Paradigm. *Statistical Science* **28**. arXiv:1312.6536 [stat].
- DINH, L., SOHL-DICKSTEIN, J. and BENGIO, S. (2016). Density estimation using Real NVP. In *Proceedings of the 5th International Conference on Learning Representations, ICLR 2017*. arXiv: 1605.08803.
- DURKAN, C., BEKASOV, A., MURRAY, I. and PAPAMAKARIOS, G. (2019). Neural Spline Flows. In *Proceedings of the 33rd Conference on Neural Information Processing Systems, NeurIPS 2019*. arXiv: 1906.04032.
- FRIEL, N. and PETTITT, A. N. (2008). Marginal Likelihood Estimation via Power Posteriors. *Journal of the Royal Statistical Society. Series B (Statistical Methodology)* **70** 589–607. Publisher: [Royal Statistical Society, Wiley].
- GELMAN, A., CARLIN, J. B., STERN, H. S., DUNSON, D. B., VEHTARI, A. and RUBIN, D. B. (2015). *Bayesian Data Analysis*, 3 ed. Chapman and Hall/CRC, New York.

- GIORDANO, R., BRODERICK, T. and JORDAN, M. I. (2018). Covariances, robustness, and variational Bayes. *Journal of Machine Learning Research* **19** 1–49. arXiv: 1709.02536.
- GIORDANO, R., LIU, R., JORDAN, M. I. and BRODERICK, T. (2022). Evaluating Sensitivity to the Stick-Breaking Prior in Bayesian Nonparametrics. *Bayesian Analysis* -1 1–67. Publisher: International Society for Bayesian Analysis.
- GIORGI, E. and DIGGLE, P. J. (2015). On the inverse geostatistical problem of inference on missing locations. *Spatial Statistics* **11** 35–44.
- GRÜNWARD, P. and OMMEN, T. V. (2017). Inconsistency of Bayesian Inference for Misspecified Linear Models, and a Proposal for Repairing It. *Bayesian Analysis* **12** 1069–1103. Publisher: International Society for Bayesian Analysis.
- HAINES, R. A. (2016). Simultaneous Reconstruction of Spatial Frequency Fields and Field Sample Locations, PhD thesis, University of Oxford.
- HENSMAN, J., FUSI, N. and LAWRENCE, N. D. (2013). Gaussian Processes for Big Data. In *Proceedings of the 29th Conference, of Uncertainty in Artificial Intelligence, UAI 2013* 282–290. arXiv: 1309.6835.
- HENSMAN, J., MATTHEWS, A. and GHARAMANI, Z. (2015). Scalable Variational Gaussian Process Classification. In *Proceedings of the 18th International Conference on Artificial Intelligence and Statistics, AISTATS 2015*. arXiv: 1411.2005.
- HOFFMAN, M. D. and GELMAN, A. (2014). The No-U-Turn Sampler: Adaptively Setting Path Lengths in Hamiltonian Monte Carlo. *Journal of Machine Learning Research* **15** 1593–1623.
- JACOB, P. E., O’LEARY, J. and ATCHADÉ, Y. F. (2020). Unbiased Markov chain Monte Carlo methods with couplings. *Journal of the Royal Statistical Society: Series B (Statistical Methodology)* **82** 543–600. arXiv: 1708.03625 Publisher: Wiley.
- JACOB, P. E., MURRAY, L. M., HOLMES, C. C. and ROBERT, C. P. (2017). Better together? Statistical learning in models made of modules. arXiv: 1708.08719 Pages: 1-31.
- JOURNAL, A. G. and HUIJBREGTS, C. J. (1978). *Mining Geostatistics*. Academic Press.
- LAO, J. and LOUF, R. (2020). Blackjax: A sampling library for JAX.
- LAO, J., SUTER, C., LANGMORE, I., CHIMISOV, C., SAXENA, A., SOUNTSOV, P., MOORE, D., SAUROUS, R. A., HOFFMAN, M. D. and DILLON, J. V. (2020). tfp.mcmc: Modern Markov Chain Monte Carlo Tools Built for Modern Hardware. arXiv:2002.01184 [cs, stat].
- LIU, F., BAYARRI, M. J. and BERGER, J. O. (2009). Modularization in Bayesian analysis, with emphasis on analysis of computer models. *Bayesian Analysis* **4** 119–150. ISBN: 1936-0975.
- LIU, Y. and GOUDIE, R. J. B. (2021). Generalized Geographically Weighted Regression Model within a Modularized Bayesian Framework. arXiv: 2106.00996.
- LIU, Y. and GOUDIE, R. J. B. (2022a). Stochastic approximation cut algorithm for inference in modularized Bayesian models. *Statistics and Computing* **32** 7. arXiv: 2006.01584.
- LIU, Y. and GOUDIE, R. J. B. (2022b). A General Framework for Cutting Feedback within Modularized Bayesian Inference. arXiv:2211.03274 [math, stat].
- LLOYD, C., GUNTER, T., OSBORNE, M. and ROBERTS, S. (2015). Variational Inference for Gaussian Process Modulated Poisson Processes. In *Proceedings of the 32nd International Conference on Machine Learning* 1814–1822. PMLR ISSN: 1938-7228.
- MAO, H., MARTIN, R. and REICH, B. (2022). Valid model-free spatial prediction. arXiv:2006.15640 [math, stat].
- MCINTOSH, A. (1963). A new approach to Middle English dialectology. *English Studies* **44** 1–11. Publisher: Routledge.
- MCINTOSH, A., SAMUELS, M. L. and BENSKIN, M. (1986). *A Linguistic Atlas of Late Mediaeval English*. Aberdeen University Press, Aberdeen.
- NICHOLLS, G. K., LEE, J. E., WU, C.-H. and CARMONA, C. U. (2022). Valid belief updates for prequentially additive loss functions arising in Semi-Modular Inference. arXiv:2201.09706 [stat].
- ORTON, H. and DIETH, E. (1962). *Survey of English Dialects*. University of Leeds Google-Books-ID: FqJzgEACAAJ.
- PERRONE, V., SHEN, H., ZOLIC, A., SHCHERBATYI, I., AHMED, A., BANSAL, T., DONINI, M., WINKELMOLEN, F., JENATTON, R., FADDOUL, J. B., POGORZELSKA, B., MILADINOVIC, M., KENTHAPADI, K., SEEGER, M. and ARCHAMBEAU, C. (2020). Amazon SageMaker Automatic Model Tuning: Scalable Black-box Optimization Technical Report, Amazon. arXiv: 2012.08489.
- PLUMMER, M. (2015). Cuts in Bayesian graphical models. *Statistics and Computing* **25** 37–43.
- POMPE, E. and JACOB, P. E. (2021). Asymptotics of cut distributions and robust modular inference using Posterior Bootstrap. arXiv: 2110.11149.
- QUIÑONERO-CANDELA, J. and RASMUSSEN, C. E. (2005). A unifying view of sparse approximate Gaussian process regression. *Journal of Machine Learning Research* **6** 1939–1959.

- RASMUSSEN, C. E. and WILLIAMS, C. K. I. (2005). *Gaussian Processes for Machine Learning*.
- SALINAS, D., SEEGER, M., KLEIN, A., PERRONE, V., WISTUBA, M. and ARCHAMBEAU, C. (2022). Syne Tune: A Library for Large Scale Hyperparameter Tuning and Reproducible Research. In *Proceedings of the First International Conference on Automated Machine Learning 16/1–23*. PMLR ISSN: 2640-3498.
- SAVITSKY, T., VANNUCCI, M. and SHA, N. (2011). Variable Selection for Nonparametric Gaussian Process Priors: Models and Computational Strategies. *Statistical Science* **26**.
- SNOEK, J., LAROCHELLE, H. and ADAMS, R. P. (2012). Practical Bayesian Optimization of Machine Learning Algorithms. In *Advances in Neural Information Processing Systems* **25**. Curran Associates, Inc.
- TITSIAS, M. (2009). Variational Learning of Inducing Variables in Sparse Gaussian Processes. In *Proceedings of the 12th International Conference on Artificial Intelligence and Statistics, AISTATS 2009* (D. VAN DYK and M. WELLING, eds.) **5** 567–574. PMLR, Hilton Clearwater Beach Resort, Clearwater Beach, Florida USA. Series Title: Proceedings of Machine Learning Research.
- WASSER, S. K., SHEDLOCK, A. M., COMSTOCK, K., OSTRANDER, E. A., MUTAYOBA, B. and STEPHENS, M. (2004). Assigning African elephant DNA to geographic region of origin: Applications to the ivory trade. *Proceedings of the National Academy of Sciences* **101** 14847–14852. Publisher: Proceedings of the National Academy of Sciences.
- WASSER, S. K., MAILAND, C., BOOTH, R., MUTAYOBA, B., KISAMO, E., CLARK, B. and STEPHENS, M. (2007). Using DNA to track the origin of the largest ivory seizure since the 1989 trade ban. *Proceedings of the National Academy of Sciences* **104** 4228–4233. Publisher: Proceedings of the National Academy of Sciences.
- WILLIAMSON, K. (2008). A Linguistic Atlas of Older Scots, Phase 1: 1380-1500. url: <https://www.lel.ed.ac.uk/ihd/laos1/laos1.html>.
- YU, X., NOTT, D. J. and SMITH, M. S. (2021). Variational inference for cutting feedback in misspecified models. arXiv: 2108.11066.
- ZHANG, T. (2006). Information-theoretic upper and lower bounds for statistical estimation. *IEEE Transactions on Information Theory* **52** 1307–1321. Conference Name: IEEE Transactions on Information Theory.
- ZHUANG, J., TANG, T., DING, Y., TATIKONDA, S., DVORNEK, N., PAPADEMETRIS, X. and DUNCAN, J. S. (2020). AdaBelief Optimizer: Adapting Stepsizes by the Belief in Observed Gradients. arXiv:2010.07468 [cs, stat].
- ÁLVAREZ, M. A., ROSASCO, L. and LAWRENCE, N. D. (2012). Kernels for Vector-Valued Functions: A Review. *Foundations and Trends in Machine Learning* **4** 195–266. arXiv: 1106.6251.